Fermi National Accelerator Laboratory

TM-1193

The TEVATRON Muon Beam:

A High Intensity Beam with Well Defined Polarization

A. Malensek and J. G. Morfín
Fermi National Accelerator Laboratory
P.O. Box 500, Batavia, Illinois 60510

July 1983

Operated by Universities Research Association Inc. under contract with the United States Department of Energy

1. Description and Philosophy

Note: This report contains references to the term "WBS". It is included because this technical memo is taken from a more detailed report submitted to the Department of Energy. For that report, each subsection contains WBS numbers and letters that are used by the DOE for accouting purposes.

1.1 Introduction

The previous muon beam at Fermilab was obtained by redirecting the secondaries from the neutrino target without attempting to refine the resulting muon beam. This non-dedicated muon beam presented the experimenter with several non-negligible problems. Upon considering the physics aims of the Tevatron era, it was deemed necessary to construct a new muon beam which would be designed specifically to meet the desired goals. The first attempt[1] to design a high intensity Tevatron muon beam was undertaken by R. Evans et al. Much useful information was contained in that study, particularly concerning halo spoilers, and served as a basis for the present work.

Presently there are two Tevatron muon experiments with stage II approval. Of the two approved experiments; one (E640)[2] will involve the Multimuon Spectrometer and the other (E665)[2] will combine the superconducting Chicago Cyclotron Magnet with the European Muon Collaborations Vertex Detector (Streamer Chamber within a superconducting magnet plus associated counters). Integrating the requirements of the two proposals, the muon beam must have the following capabilities.

1. Intensity (μ^+) $\geq 3.0 \times 10^6$ / beam spill sec. at $x \geq 0.5$, where $x = E_\mu$/Proton energy.

2. Halo*μ / Beam μ less than 0.1 at the experiment

3. Incoming muon momentum known to within 0.5% by momentum tagging.

4. Hadron contamination within the muon beam $< 10^{-7}$

5. Limited spatial and momentum spread of the beam at the experiment.

Furthermore, to enable the precise measurment of the important weak-electromagnetic interference effects, as well as to study polarized μ - polarized N interactions:

6. For a given P_μ the associated polarization (λ) must be known to less than 0.1 ($\Delta\lambda \leq 0.1$ over the range $-0.9 \leq \lambda \leq 0.9$).

7. The intensity of the beam meeting requirement 6 must be maximized.

With these goals in mind, and using the earlier results contained in TM-754 as a basis, a new beamline has been designed.

* The definition of "halo" used in this report is an untagged muon entering the detector within $\pm$ 1.5 m of the nominal beam center.

1.2 The Beam Elements

To describe the resultant solution, it is convenient to divide the beam into four major sections; i) pretarget, ii) target and front-end elements, iii) parent (decay) FODO and iv) muon FODO. It was determined that no single fixed beam configuration could meet all of the above requirements. However, a bimodel solution has been found which employs the same parent and muon FODO's and requires mainly transverse movement ($\leq 8"$) of the targeting and front-end elements. A switch is introduced in the pretarget section which steers the protons into the targeting section when it is in either its high intensity (HI) mode or its precise polarization (POL) mode. Figure 8.1-1 shows the relative lengths of the sections of the beam as well as the layout with respect to the geography of the site.

1.3 Pretarget

The path of protons in the pretarget section is identical to that laid out in TM-796 (R. Evans & T. Kirk)[3] up to a point in Enclosure G2. At this point, protons intended for the HI mode are bent 0.188 m Radians west ($\theta = -29.452$) while protons for the POL

mode are bent at 0.188 m Radians east (θ = -29.828). Since there is such a small angle between the proton paths when operating in one mode or the other, it seems economical to perform the mode switch with MUBEND which is located in G2. MUBEND is rotated about 16°, so a change in horizontal angle always implies a change in vertical angle. The vertical trim in G2 can be used to correct the slight vertical steering introduced when MUBEND is changed from one mode to the other. The protons continue along their respective path until Z = 3620 where they enter the combined pretarget - target - front-end enclosure MUHALL. A doublet consisting of 5 quadrupoles focuses the protons on the target located ~ 225 ft. downstream. These quadrupoles, as well as a vertical bend, which levels off the beam at Y = 733', are utilized by both HI and POL modes.

For radiation safety reasons, this depth of 10 ft underground is maintained for the complete beamline up to the experimental hall (MULAB). The pretarget section of the HI mode has, in addition, 30 ft. of bend which steers the protons 4.03 m Radians to the east to enable a match of the two modes at the start of the parent FODO. The doublet quadrupoles are arranged FFDDD. This configuration minimizes the divergence in the bending plane of the secondary beam and maximizes the spatial separation of the desired secondaries and the primary protons at the beam dumps.

1.4 Target and Front End Elements

The protons have now arrived at the targeting position:

	HI	POL
x	-45.559	-46.029
z	3842.5	3842.5
θ	-33.483 m Radians	-29.828 m Radians

Note that the target assembly, which consists of the target followed directly by two bends (133 KG-m), must be movable.

The first beam dump is encountered after 34 feet of drift space. Off-momentum secondaries are dumped here as shown in Figure 8.1-2. All secondaries with ΔP/P less than -40% as well as the primary 1 Tev protons, for secondary tunes of $x \leq 0.6$ are stopped at this point. The general scheme, for dumping the 1 TeV protons is summarized in Figure 8.1-3. For 700 GeV the dump has to be retracted from its 600 GeV position. To increase the acceptance for low momentum tunes, it is also necessary to move it further away from the optic axis. The difference between the trajectories of the HI beam and the POL beam is - 3" at the upstream end of the dump and - 2" at the downstream end. Movement of the dump jaws 1" to the east and 4" to the west from the nominal axis of the POL Beam is sufficient to accomodate both beams.

Both modes now share the secondary gathering elements which consist of six quadrupole magnets arranged in a doublet (FFF DDD). This arrangement collects as many pions and kaons in as large a momentum band as possible. It compares favorably with the other major alternative, a triplet, because the magnification in the doublet scheme is similar to the magnification of the triplet scheme. The doublet scheme, which introduces strong bends directly after the target followed by a dump, has the additional feature of reducing the radiation absorbed by the quadrupoles. This alleviates the problem of extra shielding, surrounding most of the quadrupoles, and a long bathtub that the triplet scheme would require.

The large $\int B\,dl$ immediately following the target, combined with the magnetic elements downstream of the dump causes the POL beam to have a double valued x vs p correlation at the momentum collimator. (See Figure 8.1-5) The low momentum band can be eliminated by making $\int B\,dl$ for the first bends as large as possible and then making a cut on the low momentum side with the dump aperture. With the geometry of this beam, 17.5 kg in each of the first bends, and a dump that cuts particles greater than - 1" from the optic axis (on the low momentum side) is sufficient to eliminate this second band. However, this is only true for parent particles; this passive dump is ineffective in stopping the muons.

Thus the second band will still be populated by muons that are produced upstream of the dump. Those muons that are accepted from one band will have different polarizations from those in the other band resulting in an increased $\Delta\lambda$. For the forward POL beam at 500 GeV, the relative number of accepted muons from each band is heavily weighted in favor of the high momentum band and therefore affects $\Delta\lambda$ very little. However, the backward POL beam is quite different since the weighting becomes unfavorable. The high momentum band is now being populated by 800 GeV parents, which are scarce when compared to 600 and 500 GeV parents, which populate the low momentum band. This leads to a significant increase in $\Delta\lambda$. The unwanted muons are eliminated by magnetically removing them from the acceptance with a magnetic collimator. The effect of the magnetic jaw at 15 kg and different field orientations is shown in Figure 8.1-6. The number of uncorrelated muons is significantly reduced when an east or west bending magnetic collimator is used.

After the doublet, the beam operated in the HI mode is parallel and is matched into the FODO. The POL mode is somewhat more complicated since a restricted momentum bite is necessary. The gathering doublet serves, in this mode, to focus the secondaries on a collimator. The secondaries are subjected to 97 KG-m of bend, located between the F and D elements of the doublet, to

introducee a large dx/dp component. A collimator located 235 feet from the bend point, in the first FODO enclosure, selects the required momentum range. It was determined that to meet design goal 6, a $\pm$ 0.8" slit would be sufficient. (See Figure 8.1-4)

Along with the collimator, there is a second dump and a quadrupole located in the first FODO enclosure. The 1 TeV protons are dumped here for secondary tunes of $0.6 \leq X \leq 0.8$ in the HI mode and $0.6 \leq X \leq 0.9$ in the POL mode. The quadrupole is part of the FODO channel in the HI mode and acts as a field lens in the POL mode. As shown in Figure 8.1-7, the field lens is quite effective in capturing beam that would otherwise be lost.

In attempting to devise a single Beamline which would optimize the flux and satisfy the design goals for the polarization measurements, it was found that with a secondary tune of 800 GeV the POL beam with the collimator wide open gave only 36% of the flux of the HI beam while trying to use the HI beam as a polarized beam proved impossible since there is insufficient dx/dp correlation resulting in a large $\Delta\lambda$ no matter how small the collimator setting becomes.

1.5 Decay FODO

The most efficient way of transmitting a beam of particles over long distances with maximal transmission is via a periodic system referred to as a FODO. Both the ddecay FODO and the muon FODO consist of single quadrupoles spaced at equal intervals and alternate focus, defocus, focus---etc.

Three important lengths need to be fixed; the interquad length (L), the overall length (D) of the decay FODO and the length of the muon FODO. In determining these lengths, the following factors were considered:

A. Decay length of 800 GeV π's and k's.

B. Transmission efficiency of the FODO for a given interquad length

C. Phase advance per cell (shape of the beam at the experiment).

D. Halo at MULAB.

E. The number of quadrupoles and enclosures.

F. The physical positions of the various quadrupole enclosures and MULAB with respect to existing structures.

There is a phase advance associated with each pair (FD) of quadrupoles in the beam line. Maximum transmission occurs for a phase advance of 76.5°, however, since we wish to recover the original phase space of the beam at the end of the FODO a simple fraction of 180° is preferable. For both beams there is a total phase advance of 540° between the beginning of the FODO and the absorber. Since the POL mode has one less magnet in its FODO than the HI mode, this requires a phase advance per cell of 60° for HI and 63.5° for POL. Keeping the total phase advance at the absorber a multiple of 180° assures a minimum spot size in the beam. The smaller the spot on the absorber, the less the multiple scattering increases the beam phase space, and the larger the flux at MULAB. Once the choice of phase advance has been made, there

is a given relation between the field strength of the quadrupoles, the interquad distance and the momentum of the transmitted particles. Using the HI front-end the efficiency of the FODO in transmitting off momentum particles is shown in Figure 8.1-8.

The importance of factor (B) above is displayed in Figure 8.1-9. With the maximum field of the 4Q120 quadrupoles, the interquad distance is 143 ft. and the transmission is maximum. The efficiency has dropped only by 5% for L=200, but then it drops rapidly until L=500 when it starts to level off again. The dashed curve in Figure 8.1-9 corresponds to the case where the interquad distance of the muon FODO (L_μ) is held at 200 ft. while the L for the parent FODO is allowed to vary. Large losses are found to occur at the match point.

Once decisions are made on B and C, the length of the muon FODO is determined mainly by cost and $\int B\,dl$. The shape of the beam at MULAB is required to be larger horizontally than vertically since the upstream experiment takes pictures of events occurring in the horizontal plane. It is therefore natural to make the Lab position an extension of the FODO lattice, putting it at an "F" location.

After studying all of the above factors, the length of the decay FODO was chosen to be 3600' and $L_\pi = L_\mu = 200'$. At the end of the decay FODO, there is an absober/dump to absorb all hadrons (including the 1 TeV protons for $P_{\pi K} > 800$ GeV tunes) consisting of 40 ft. of beryllium, 20 ft. of which is inserted in a large aperature bending magnet. The bend allows the choice of momentum bite in $\Delta p/p$ of the muons reaching MULAB. It is also important that the absorber be placed at a "D" position in the FODO lattice. The introduction of a horizontal bend at the same location gives a much higher yield than placing it at an "F" position.

1.6 Muon FODO

In addition to the straight forward function of conveying muons from the absorber to the MULAB, the muon FODO serves the very crucial purpose of "cleansing" the muon beam which eventually reaches the experiments. The well collimated muon beam, for which the momentum is known to within 0.5%, is surrounded by a halo of muons with unknown momentum which could saturate the experiments with useless interactions. These unwanted muons must be eliminated in order to provide an efficient beam.

Due to the nature of this halo, it is impossible to absorb it. Rather, a way has been found to create a sharp magnetic edge which surrounds the muon beam and forces the halo radially outward away from the beam center. Two types of halo spoilers are employed: conventional toroids and "mupipe". The dimensions of the conventional toroids were optimized with the aim of using the toroids available on site where possible. The best results were obtained by using 30' of the 68" diameter toroid most of which already exists, plus 20' of 120" diameter toroid which must be built. A more complete list of various toroid configurations using a variety of radii is in Appenix III. To emphasize the necessity of the 120" diameter toroid, if it is replaced by more 68" diameter toroid, regardless of length, the halo to beam ratio increases by a factor of 1.8.

Mupipe is cold rolled pipe, the dimensions of which have been chosen to most efficiently rid the beam of halo. A large current (3-5kA) is fed onto the inner surface of the pipe at one end and returned from the other end via a cable. The pertinent dimensions - length, inner radius, and wall thickness - were determined using the program HALO[4]. Of the three dimensions, it was found that the length of the pipe was only weakly correlated to the other two dimensions while the most sensitive was the wall thickness. The inner radius was chosen so as to cut minimally into the beam and

to provide some shadowing for the following beam elements. After studies (summarized in Figure 8.1-10) the length and wall thickness were chosen to be 30' and 1.25" respectively. The furthest upstream mupipe has an OD of 7" and an ID of 4.5", the other three have an OD of 7 1/2" and an ID of 5.0. If the first is made the same as the other three, the halo increase from 5.3% to 6.5%. The 30' length gives a safety factor in the area cleared of halo at the experiment and the thickness is readily available from commercial manufacturers and need not be a special order. For fine tuning of the halo to beam ratio, the second and third 30' lengths of mupipe will be divided into four 15' lengths, each of which will be movable in the plane perpendicular to the beam. Table I shows the effectiveness of each of the mupipes. Figure 8.1-11, progressing from no spoilers to just toroids to toroids plus mupipe, demonstrates the efficiency of the halo spoilers. The introduction of toroids plus mupipes has reduced the halo/beam ratio by an order of magnitude.

The muon tagging process begins with a bend located midway between the last quadrupole enclosure and the experimental building (MULAB). The bend (73.15 KG-M) is in the same direction as the bend at the absorber and serves to cancel some of the dispersion introduced at the "absorber bend". P_μ is measured to an accuracy of 0.5% by using PWC's with a 1/2 mm wire spacing.

1.7 Further Considerations

The radiation due to the muon beam at the site boundary (Z = 16500) and at KRESS creek (Z = 12800) were estimated using HALO. The elevation as a function of Z in Figure 8.1-12 shows that beam elevation is above ground level for ~ 1500 ft in the vicinity where the beam crosses Kress Creek. For a flux of 10^8 muons per cycle and expected doubler operation of 60 seconds per cycle, 100 hours per week, 25 weeks per year, we obtain radiation rates of 0.01 mrem/hr at the Creek and 3 mrem/yr at the site boundary.

1.8 Yield

The last important factor in determining the yield of the beam in its two modes and various tunes is the relationship between flux and the momentum spread of the muons ($\Delta p/p$). As mentioned, the desired muon momentum band is selected at the absorber bend. Figure 8.1-13 shows the muon momentum spectra for the HI mode tuned for maximum P_μ and for B = 8KG at the absorber bend Figure 8.1-14 shows the beam profile at the proposed target position in MULAB. The FWHM is ~ 2 inches in x and 1 inch in y. The beam divergences at this point is $\langle y' \rangle$ = .001 mr with FWHM = 0.55 mr and, in the bend plane, $\langle x' \rangle$ = -0.58 mr with FWHM = 1.2 mr. The

momentum spectra for the POL mode tuned for forward helicity (P_π/P_μ = 500/500 GeV) and backward helicity (800/500) is displayed in Figure 8.1-15 and 8.1-16. The corresponding dependence of the polarization (λ) on P is also shown.

Although the beam has been designed and optimized to yield maximum intensity and low halo at high P , there is considerable interest in operating the beam at lower energies to match with existing data. It was found that for P_μ tunes down to 100 GeV, both modes yielded significant flux and satisfactory halo to beam ratios. The momentum spectra of the low energy tunes is shown in Figure 8.1-17.

Table II summarizes the yields of some typical tunes of the two modes.

1.9 Muon Laboratory

The last item in the new Muon beam is the Muon Laboratory Building shown in Figure 8.3-7. The building will contain two stories, one story a pit below grade approximately 60 ft by 250 ft, which will house the experimental apparatus. A second story at grade level, approximately 60 ft by 250 ft, covering the pit, will consists of a high bay above grade utilizing structural steel frame and insulated metal siding. A second portion of the above-grade structure approximately 20 ft by 250 ft will be divided into two stories and house light laboratories, counting rooms, and office space.

One of the current experiments approved to operate in the new Muon Lab will use the Chicago Cyclotron Magnet (CCM) as a spectrometer magnet and will also use a vertex detector that had previously been used by the European Muon Collaboration at CERN. The other approved experiment will use the Multi-Muon Spectrometer (MMS) that will be moved from the old Muon Lab.

References

1. Evan, R. etal., "Design Study for a High Energy Muon Beam"; TM-754; November 1977.

2. Barnes, A.V. etal., "The Multimuon Spectrometer at the Tevatron"; Proposal 640 submitted to PAC. Hasert, F.J. etal., "Muon Scattering with Hadron Detection at the Tevatron"; Proposal 665 sumitted to PAC.

3. Evans, R. and Kirk, T.: "Transport of Tevatron Energy Primary Proton Beams to Neutrino Area"; TM-796; May 26, 1978.

4. Iselin, C.; "HALO" CERN 74-17; August 29, 1974.

Table I

Elements	H/B%
All off	20.0 ± 1.0*
1 off	9.7 ± 0.8
2 off	7.4 ± 0.7
3 off	11.8 ± 0.8
4 off	6.5 ± 0.6*
1 & 2 off	11.4 ± 0.8
3 & 4 off	13.0 ± 0.9*
All on	5.3 ± 0.6

Toroids on for all conditions above.

*These are lower limits due to the fact that HALO models the toroids as having a sharp magnetic edge. When mupipe 4 is off, this assumption is invalid.

Table II

Mode	P_π GeV/c	P_μ GeV/c	$\int Q_\mu / P_{int}$	$\langle P_\mu \rangle$ GeV/c	h/μ(%)	Comment
HI	800	720	3.9×10^{-5}	600+70	5.3+0.3	B = 7.7 kG
HI	500	450	3.5×10^{-4}	405+60	3.7+0.2	B = 4.8 kG
HI	300	270	6.6×10^{-4}	250+40	3.7+1.	B = 2.9 kG
HI	100	90	1.9×10^{-4}	90+20	7.7+1.4	B = 0.96 kG
POL	800	450	2.6×10^{-6}	545+65	8.5+2.2	$-1<\lambda<0$; $\langle\Delta\lambda\rangle$ = .07
POL	500	450	8.4×10^{-5}	425+55	2.1+1.0	$0<\lambda<1$; $\langle\Delta\lambda\rangle$ = .08
POL	800	720	5.2×10^{-6}	655+79	2.6+0.5	$0<\lambda<1$; $\langle\Delta\lambda\rangle$ = 0.07

Appendix I

Halo Spoilers (EQP)

The beam contains two types of halo spoilers, toroids and mupipe.

The toroids are of conventional design and have been used in a previous FNAL experiment. The coils are wound around an iron toroidal yoke having inner radius 4.5" and an outer radius of either 12", or 60". The nominal field is 18KG with an r dependence as shown in figure 8.2-4.

The mupipes are cold rolled steel pipes. The inner radius of the first 30' is 2.25" while the following 90' (3 thirty foot sections) has inner radius 2.5". In all cases the wall thickness is 1.25". The field in the steel is:

a = inner radius

b = outer radius

Note that the rapaidy with which high fields are obtained close to

the inner surface of the pipe is directly proportional to the current (I) applied. The field as a function of r and I is displayed in Figure 8.2-5. The minimum I is that which provides sufficient field to overcome multiple scattering. That is, once a halo muon enters the mupipe, it is not allowed to multiple scatter back into the aperture. It was found that the average B for those particles which overcame multiple scattering is 10KG. A mupipe (scraper) is shown in Figure 8.2-6.

List of Modifications used in Halo

1. 4Q120 aperature was modeled to have an aperature inside the two ellipses:

2. Multiple Scattering was input for dE/dZ according to TM 786.

3. The field map for the wide gap bending magnets (MRB4) was a main ring B2 field map with a 4" x 4" aperature.

4. Particle production yields are based on FN 341.

5. The magnetic field in the mupipe as a function of the pipe radius in meters is:

   17kg (-11.0968 + 194.*r) r ≥ 0.0612 meter

   17kg (0.35 + 7.24*r) r ≥ 0.0612 meters

6. Similarly the magnetic field in the toroids is:

   18kg (1.-2018*r + 0.0082*r*r)

Appendix III

If we assume that the maximum horizontal aperture of the E665 detector is dictated by the time-of-flight hodoscope and drift planes just downstream of the CVM then ± 100" on either side of the beam should have minimum halo. The ±60" vertical aperture originally assumed is sufficient.

Figure 1 shows the growth of the integrated halo/beam as a function of the horizontal aperture (vertical aperture = ±60") for different toroid configurations. Each configuration is described by the length of μ-pipe (SCR), length of r = 12" toroid, length of r = 34" toroid and finally length of r = 60" or 72" toroid.

Solution A is what had been envisioned requiring the procurement of only the 10' of 60" toroid since we already have the 12" and 34" toroid available on-site. Within the ± 100" aperture, solution A is clearly unacceptable with an ~ 22% h/μ ratio. Figure 2 displays the halo:beam ratio within the ±100" horizontal aperture as a function of the amount of steel which would have to be obtained. The curve seems to decend quite rapidly until ~ 150 tons and then levels out. I would therefore propose that we adopt configuration F2 which consists of 20' of μ pipe, 30' of 34" toroid and 20' of 60" toroid. This solution requires about a factor of two more steel than solution A but reduces the h/μ ratio by almost a factor of three.

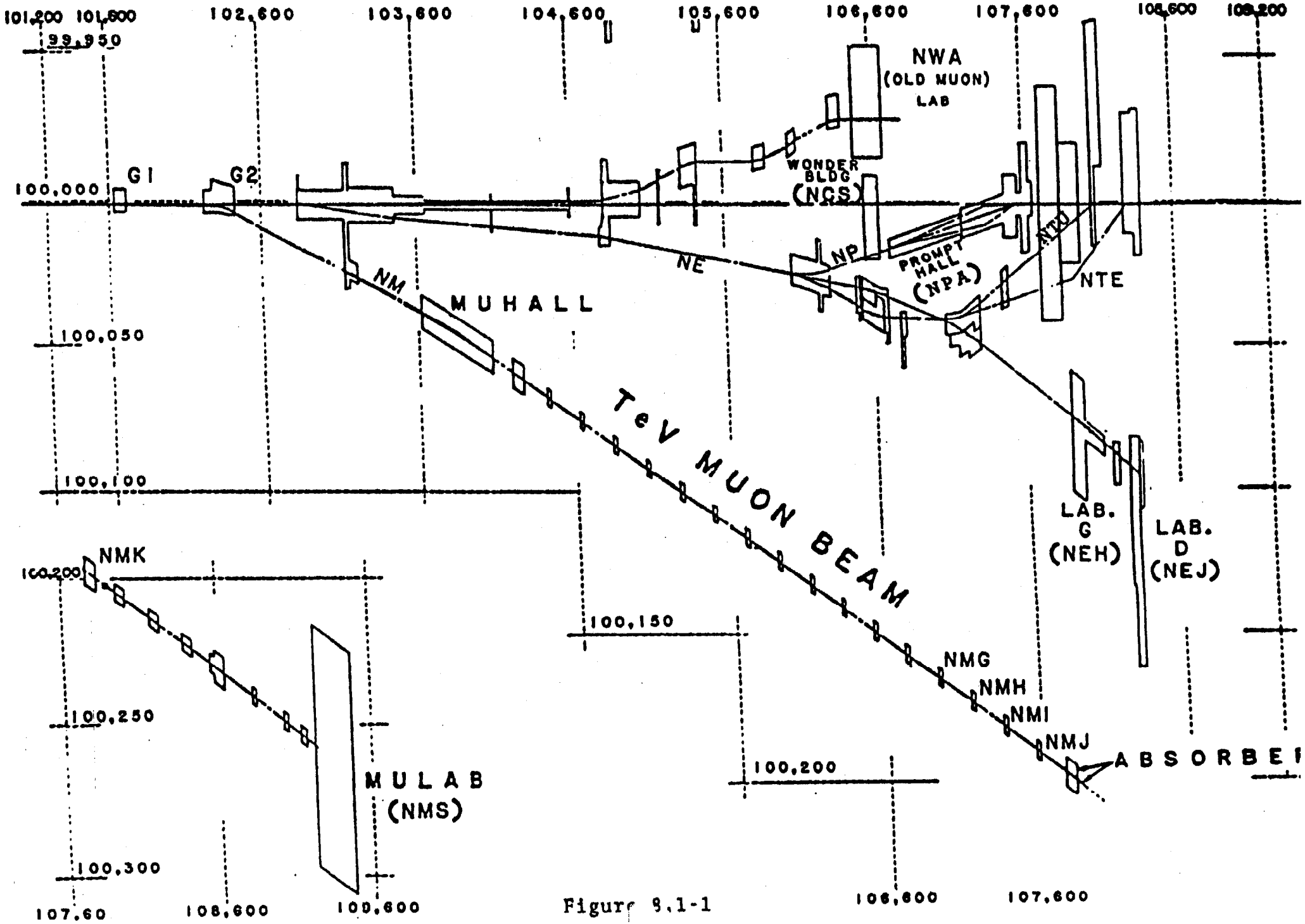
101,200
101,600
102,600
103,600
104,600
105,600
106,600
107,600
108,600
108,200
99,950
100,000
G1
G2
NWA
(OLD MUON)
LAB
WONDER
BLDG
(NCS)
NE
NP
PROMPT
HALL
(NPA)
NTE
NM
MUHALL
100,050
100,100
TeV MUON BEAM
LAB.
G
(NEH)
LAB.
D
(NEJ)
NMK
100,200
100,150
NMG
NMH
NMI
NMJ
ABSORBER
100,250
MULAB
(NMS)
100,300
100,200
107.60
108,600
100,600
106,600
107,600

Figure 3.1-1

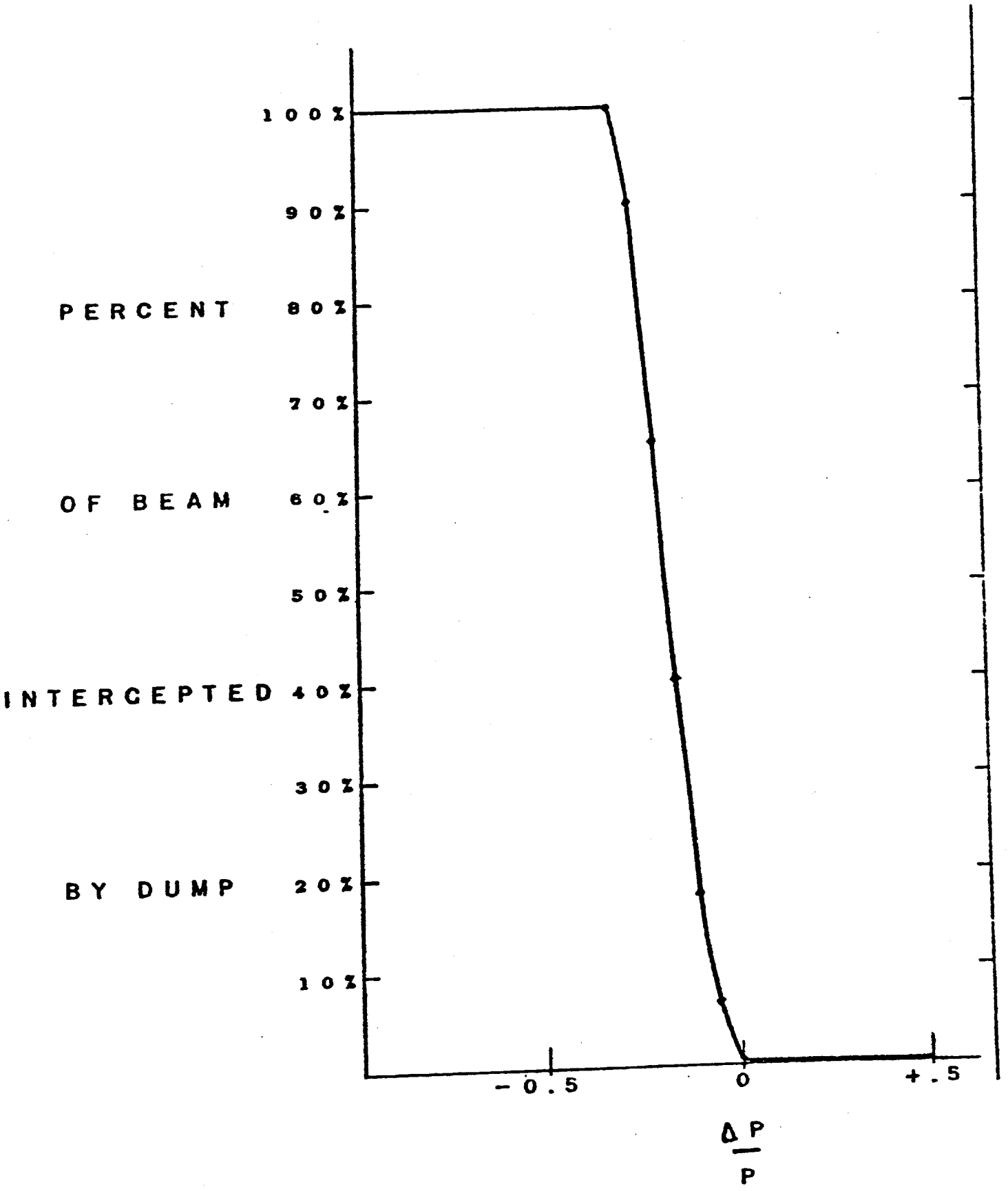
PERCENT
OF BEAM
INTERCEPTED
BY DUMP
100%
90%
80%
70%
60%
50%
40%
30%
20%
10%
-0.5
0
+.5
ΔP/P

Figure 8.1-2

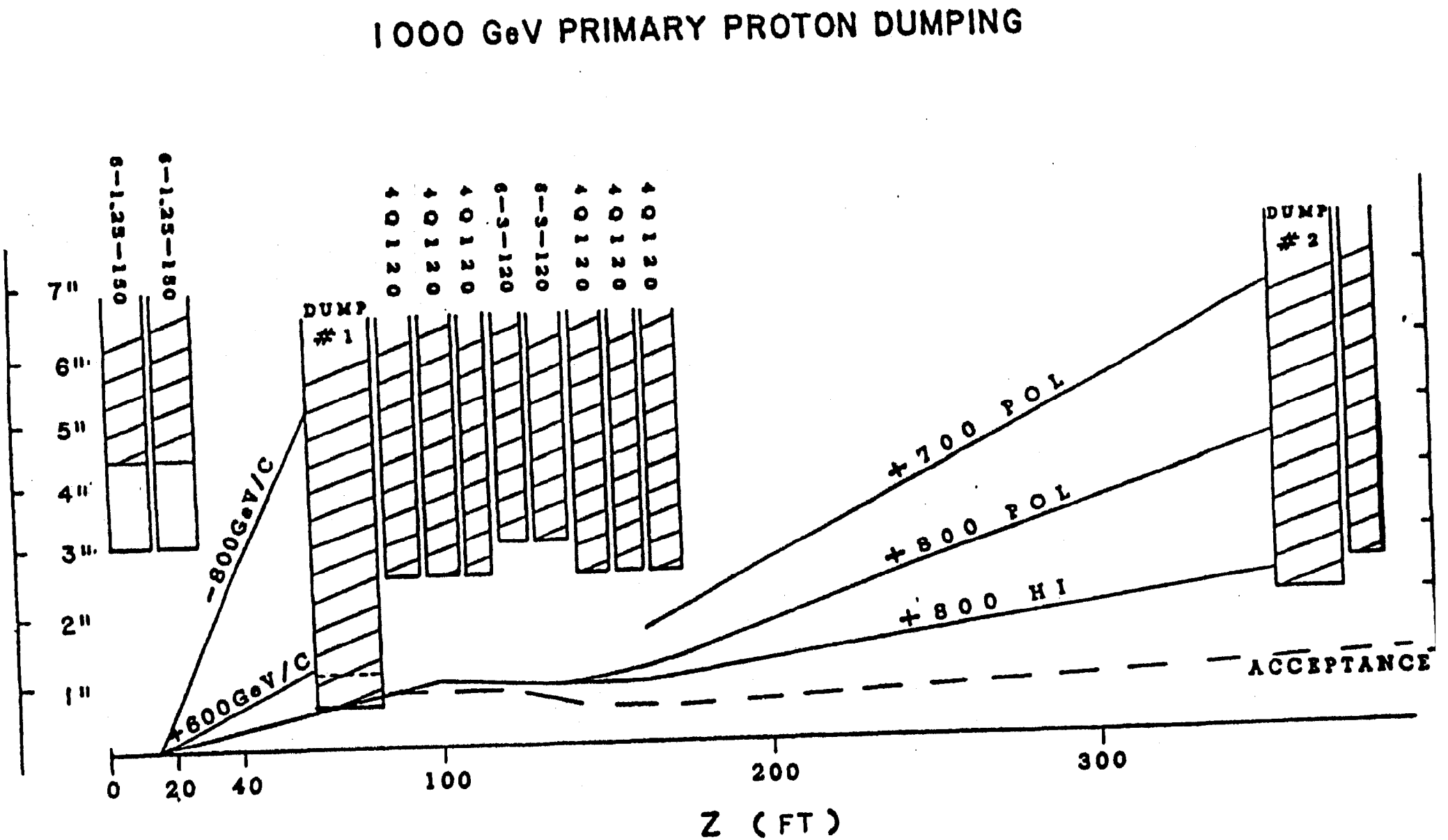
1000 GeV PRIMARY PROTON DUMPING
6-1.25-150
6-1.25-150
4-0-120
4-0-120
4-0-120
6-5-120
6-5-120
4-0-120
4-0-120
4-0-120
DUMP #1
DUMP #2
7"
6"
5"
4"
3"
2"
1"
-800GeV/C
+600GeV/C
+700 POL
+800 POL
+800 HI
ACCEPTANCE
0
20
40
100
200
300
Z (FT)

Figure 8.1.3

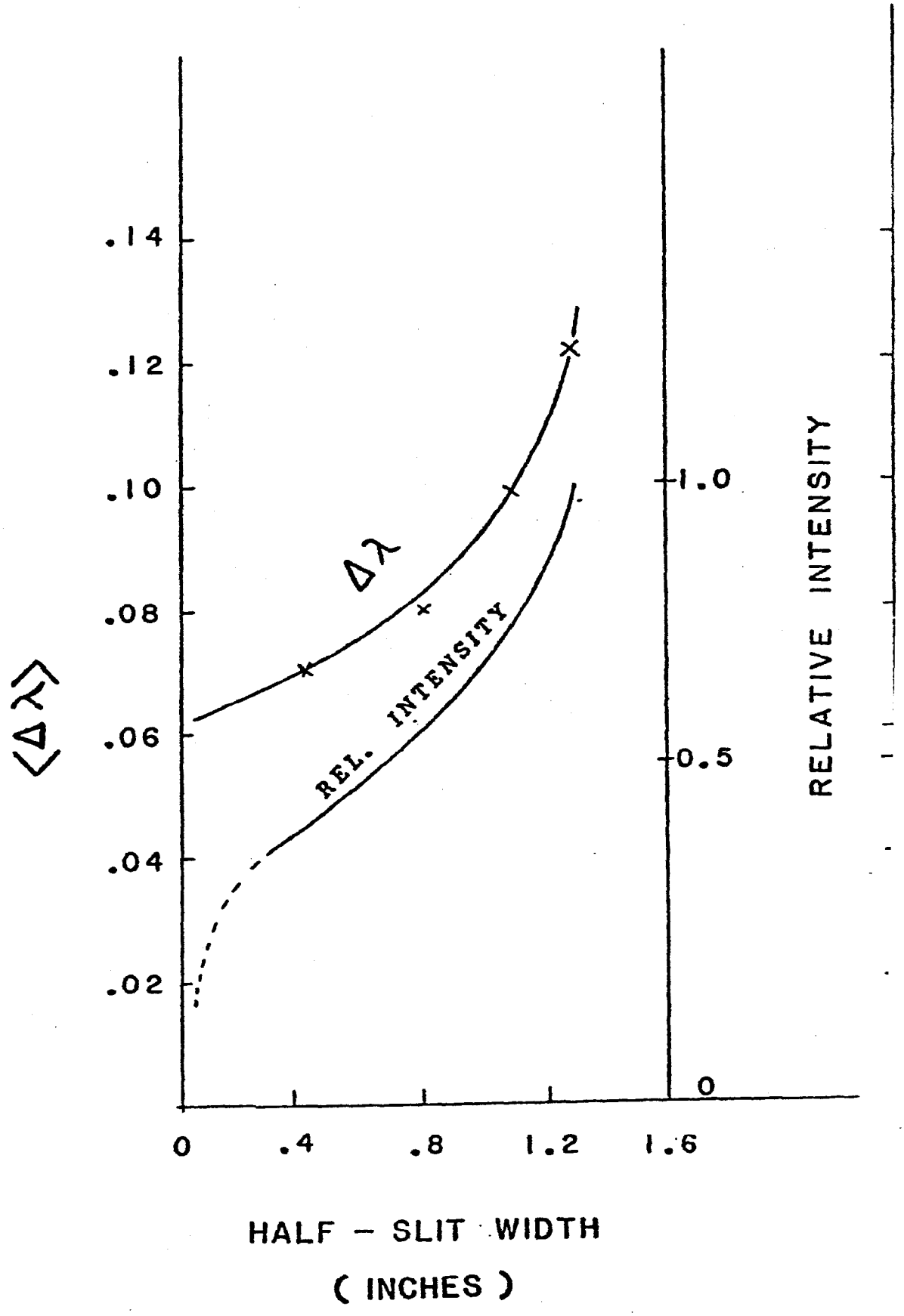
.14
.12
.10
.08
.06
.04
.02
⟨Δλ⟩
Δλ
REL. INTENSITY
1.0
0.5
0
RELATIVE INTENSITY
0
.4
.8
1.2
1.6
HALF – SLIT WIDTH
(INCHES)

Figure 8.1-4

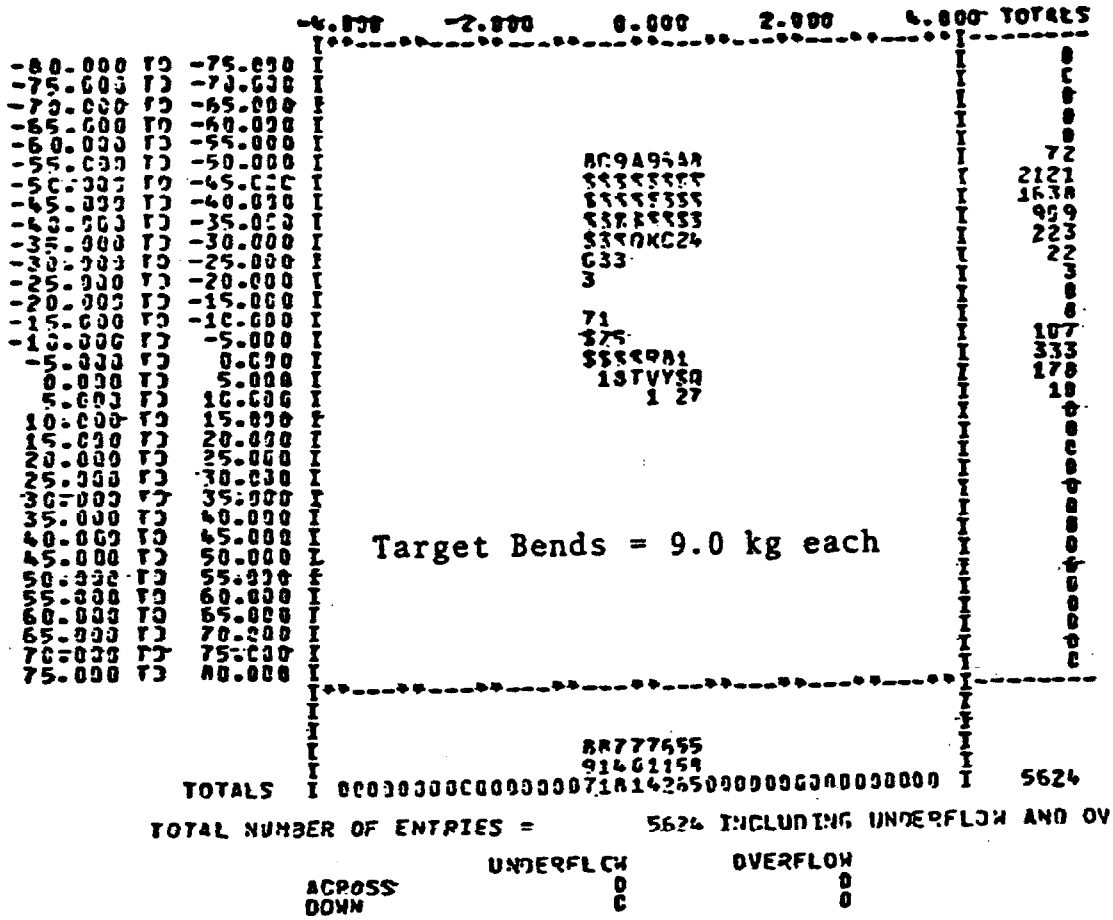

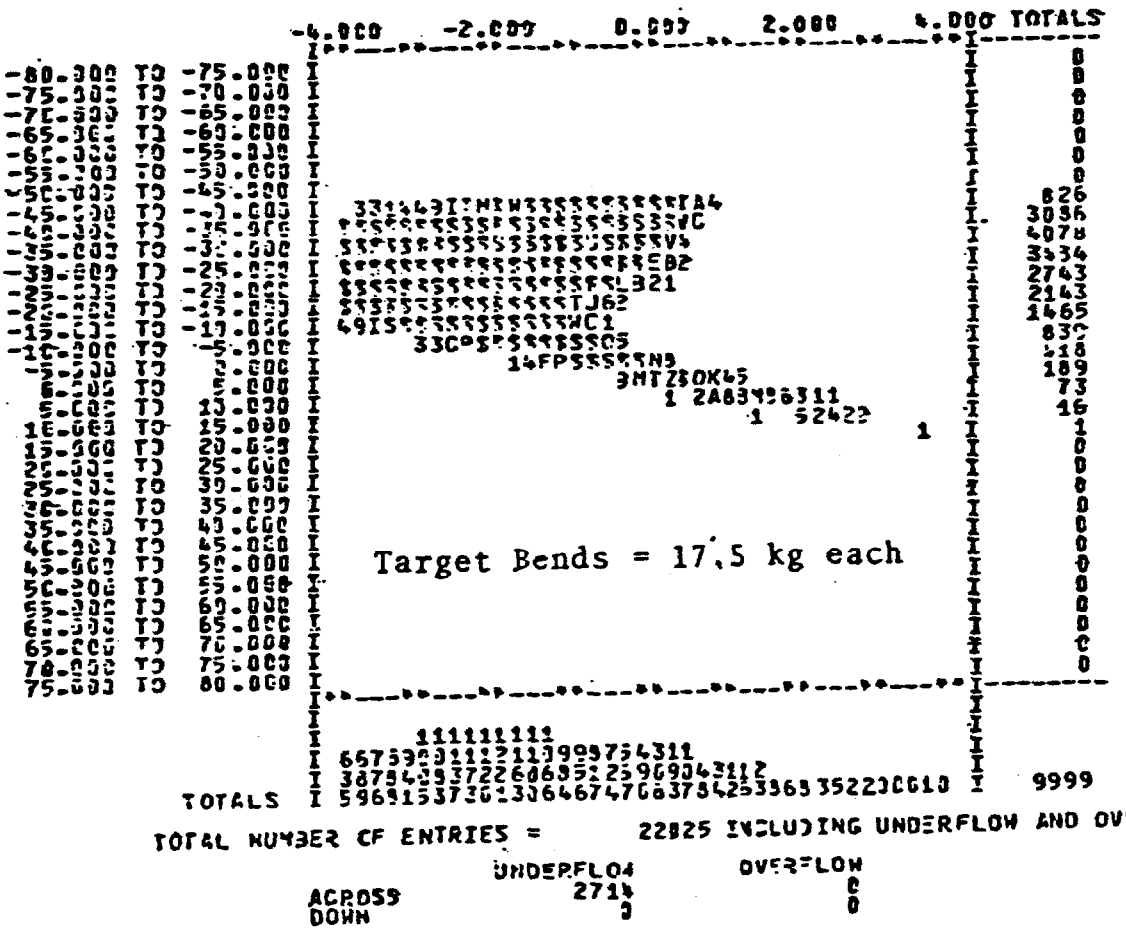

Figure 8.1-5

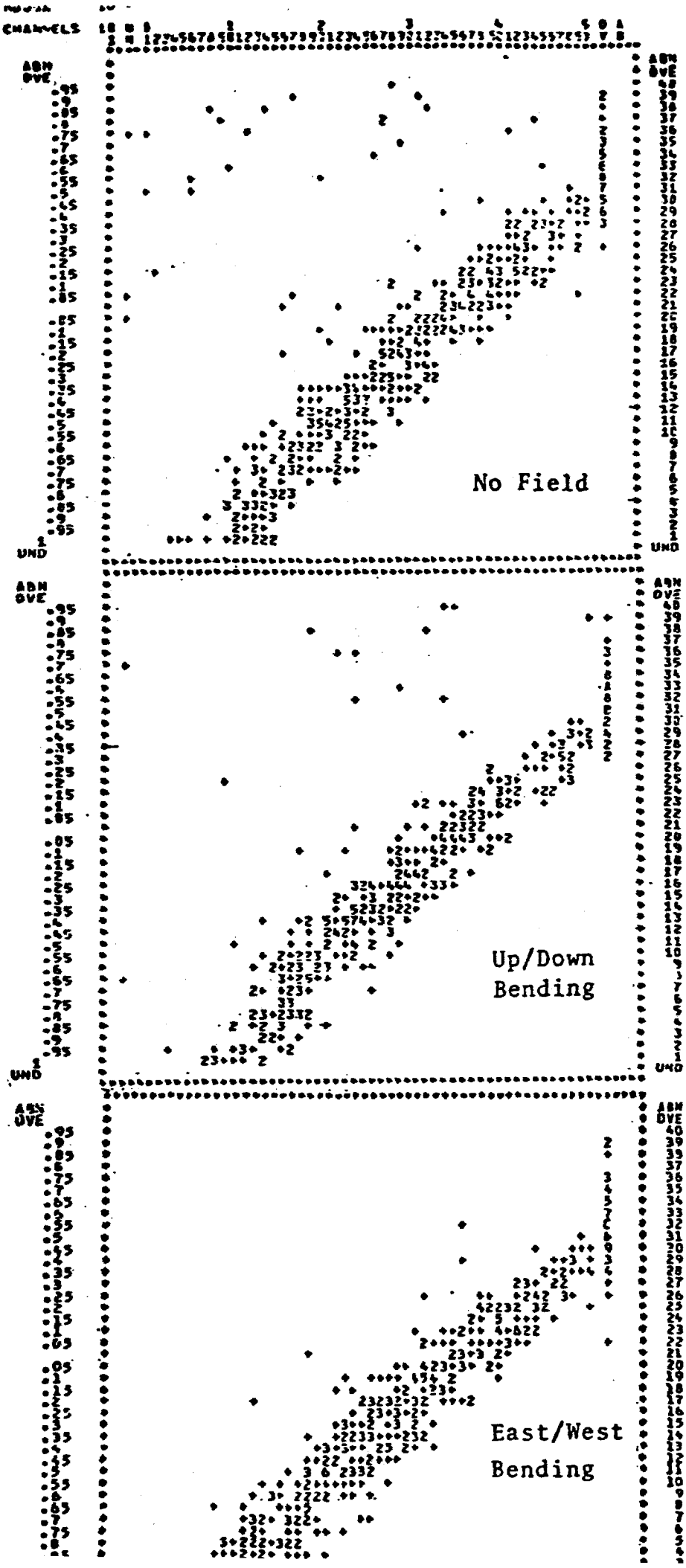

Correlation between Helicity and P for different magnetic field orientations of the magnetic collimator

Figure 8.1-6

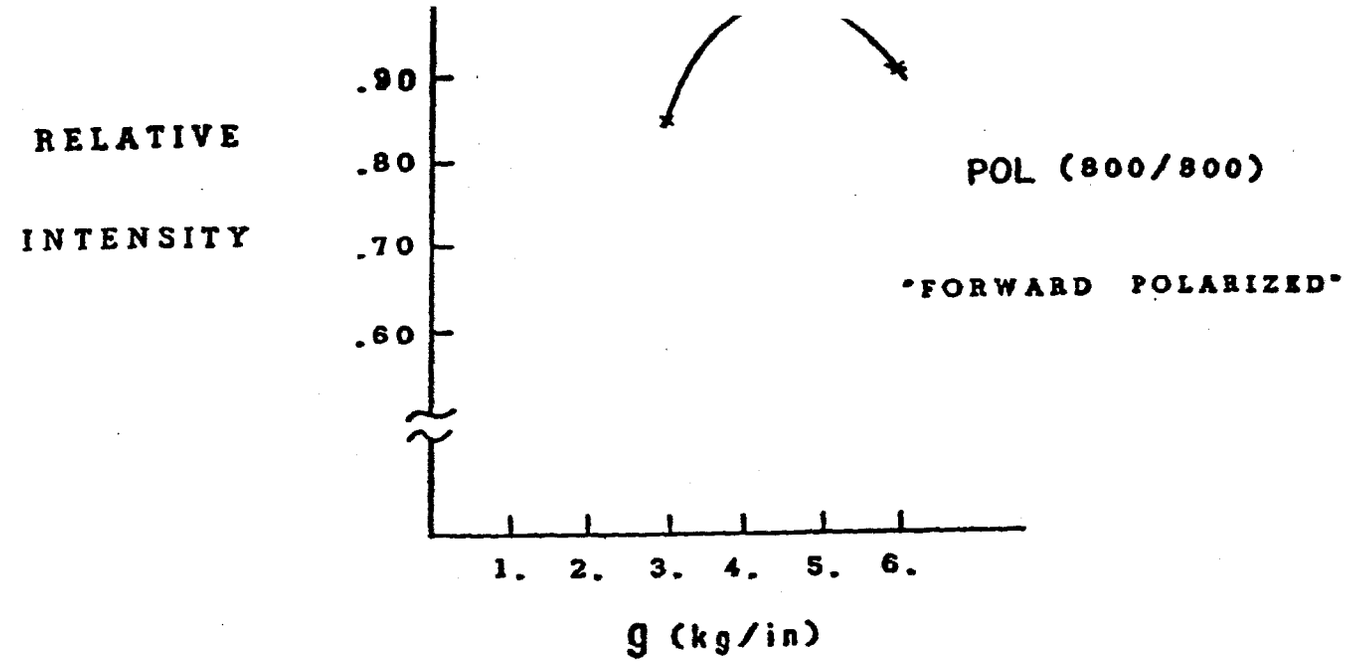
RELATIVE
INTENSITY
.90
.80
.70
.60
POL (800/800)
"FORWARD POLARIZED"
1. 2. 3. 4. 5. 6.
g (kg/in)

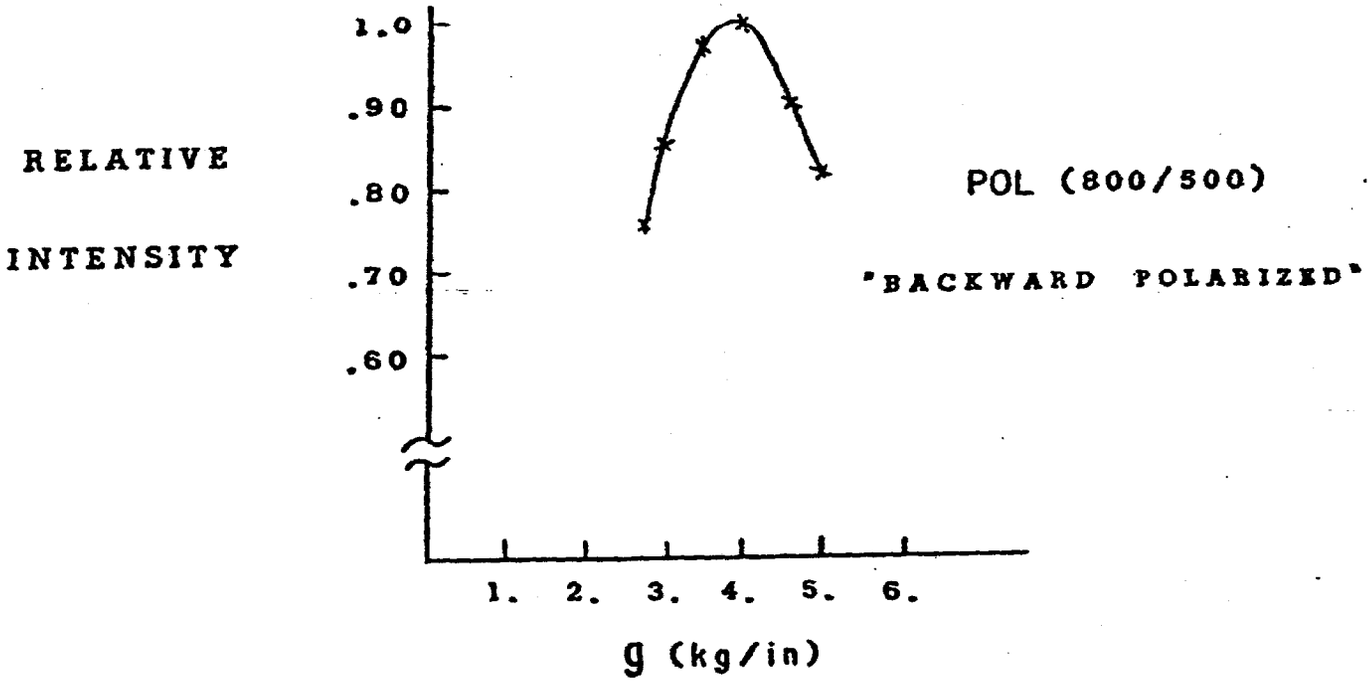
RELATIVE
INTENSITY
1.0
.90
.80
.70
.60
POL (800/500)
"BACKWARD POLARIZED"
1. 2. 3. 4. 5. 6.
g (kg/in)

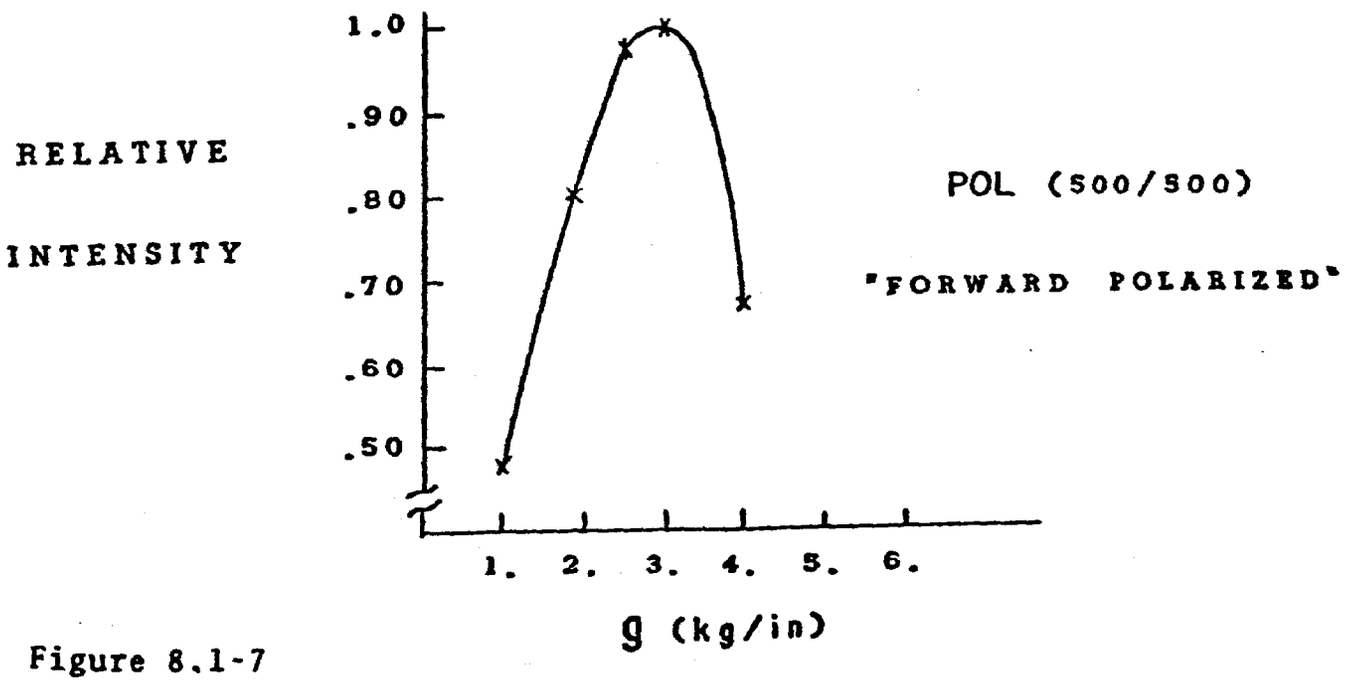
RELATIVE
INTENSITY
1.0
.90
.80
.70
.60
.50
POL (500/500)
"FORWARD POLARIZED"
1. 2. 3. 4. 5. 6.
g (kg/in)

Figure 8.1-7

EFFICIENCY OF FODO IN TRANSMITTING OFF MOMENTA PARTICLES

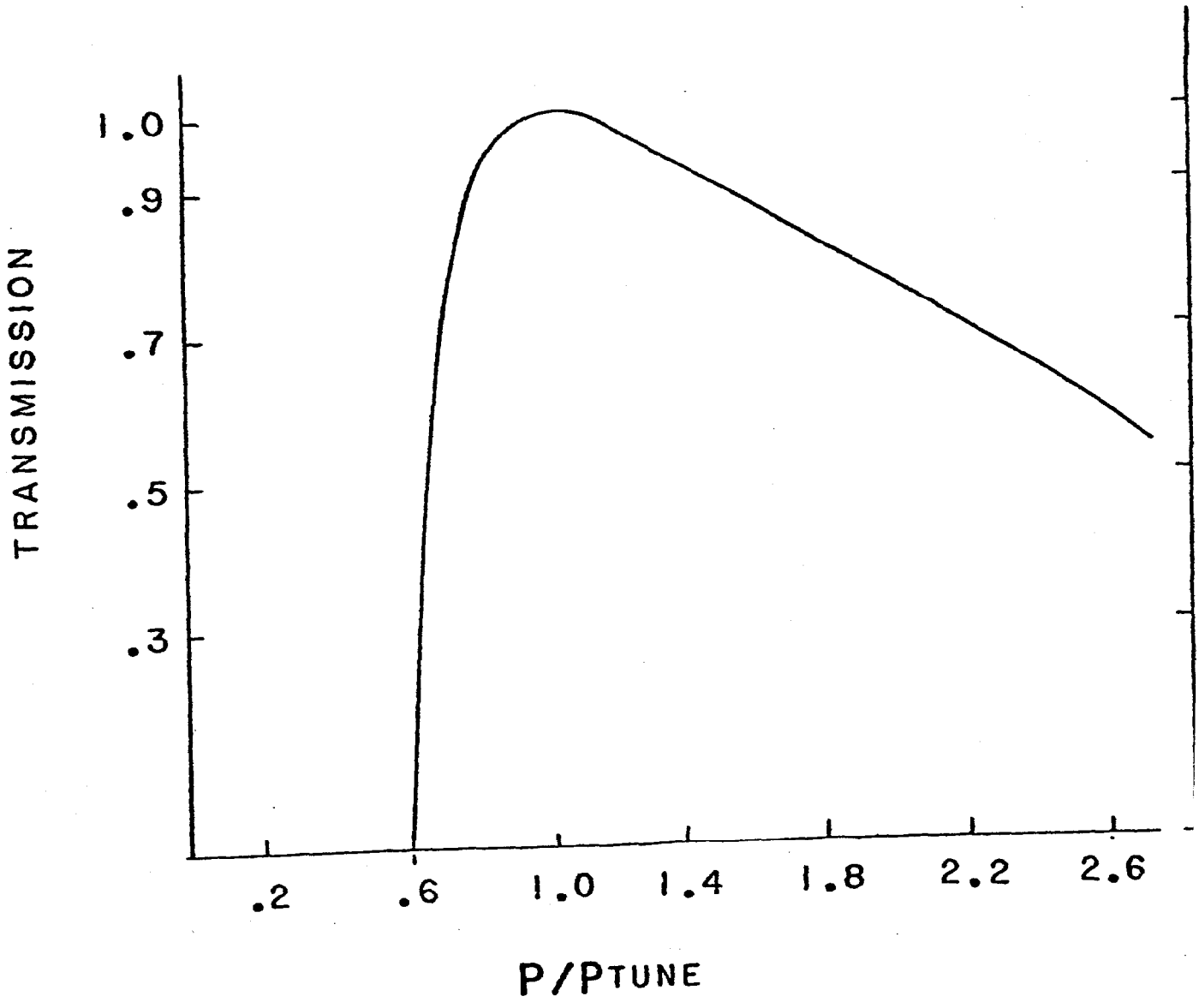

Figure 8.1-8

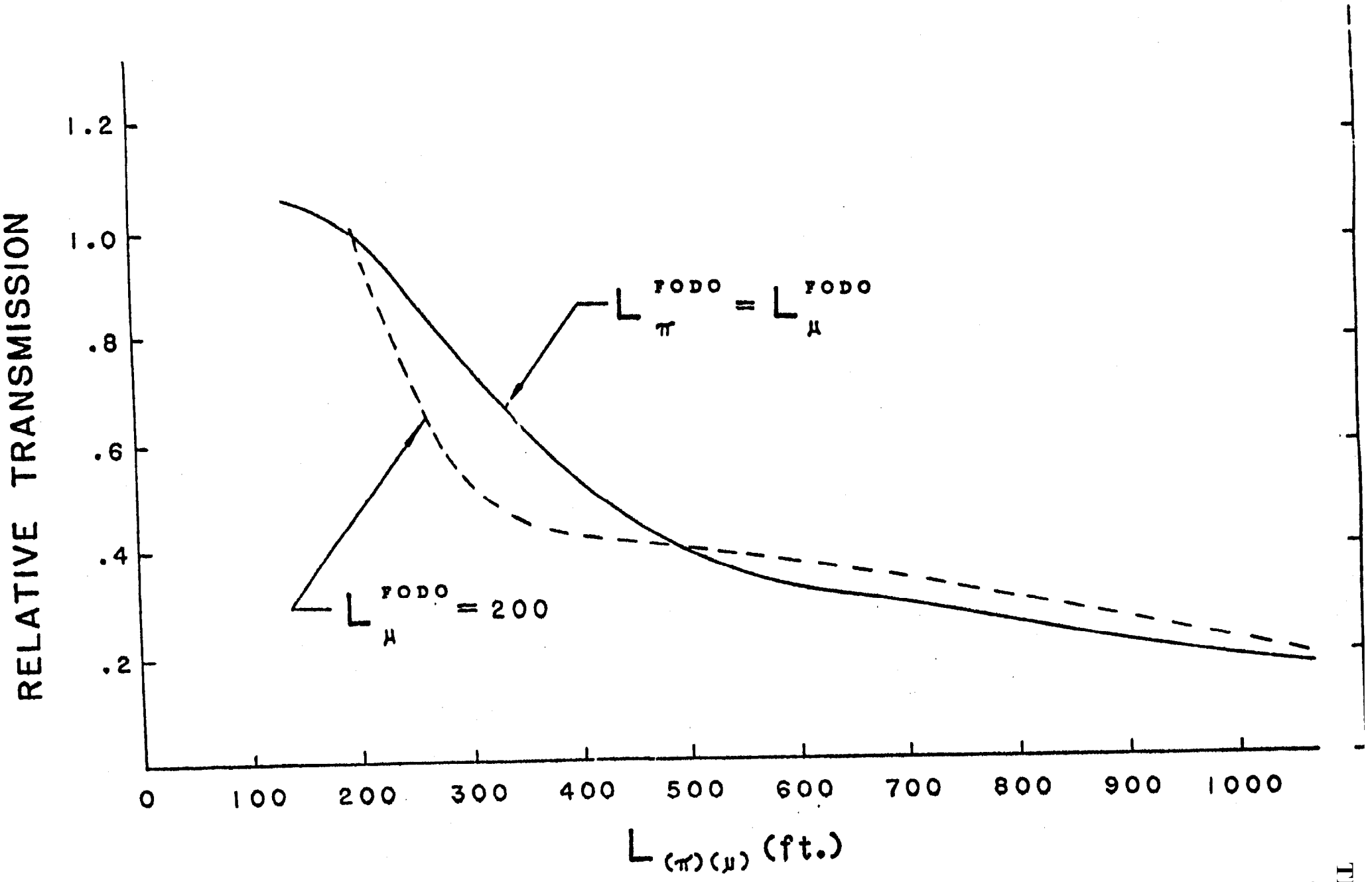
RELATIVE TRANSMISSION
1.2
1.0
.8
.6
.4
.2
0
100
200
300
400
500
600
700
800
900
1000
$L_{\pi}^{FODO} = L_{\mu}^{FODO}$
$L_{\mu}^{FODO} = 200$
$L_{(\pi)(\mu)}$ (ft.)

Figure 8.1-9

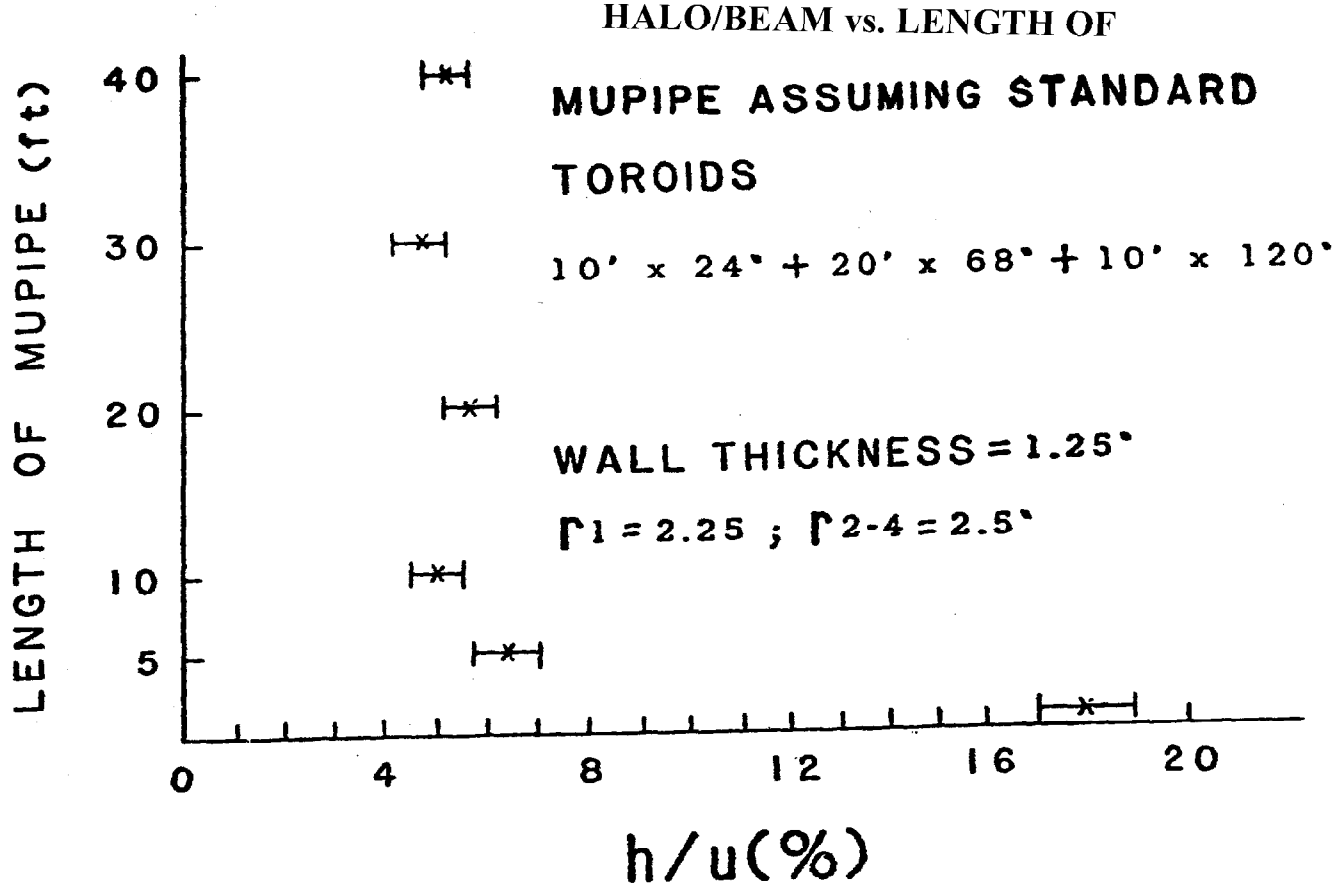
HALO/BEAM vs. LENGTH OF
MUPIPE ASSUMING STANDARD
TOROIDS
10' x 24° + 20' x 68° + 10' x 120°
WALL THICKNESS = 1.25"
r1 = 2.25 ; r2-4 = 2.5"
LENGTH OF MUPIPE (ft)
40
30
20
10
5
0
4
8
12
16
20
h/u(%)

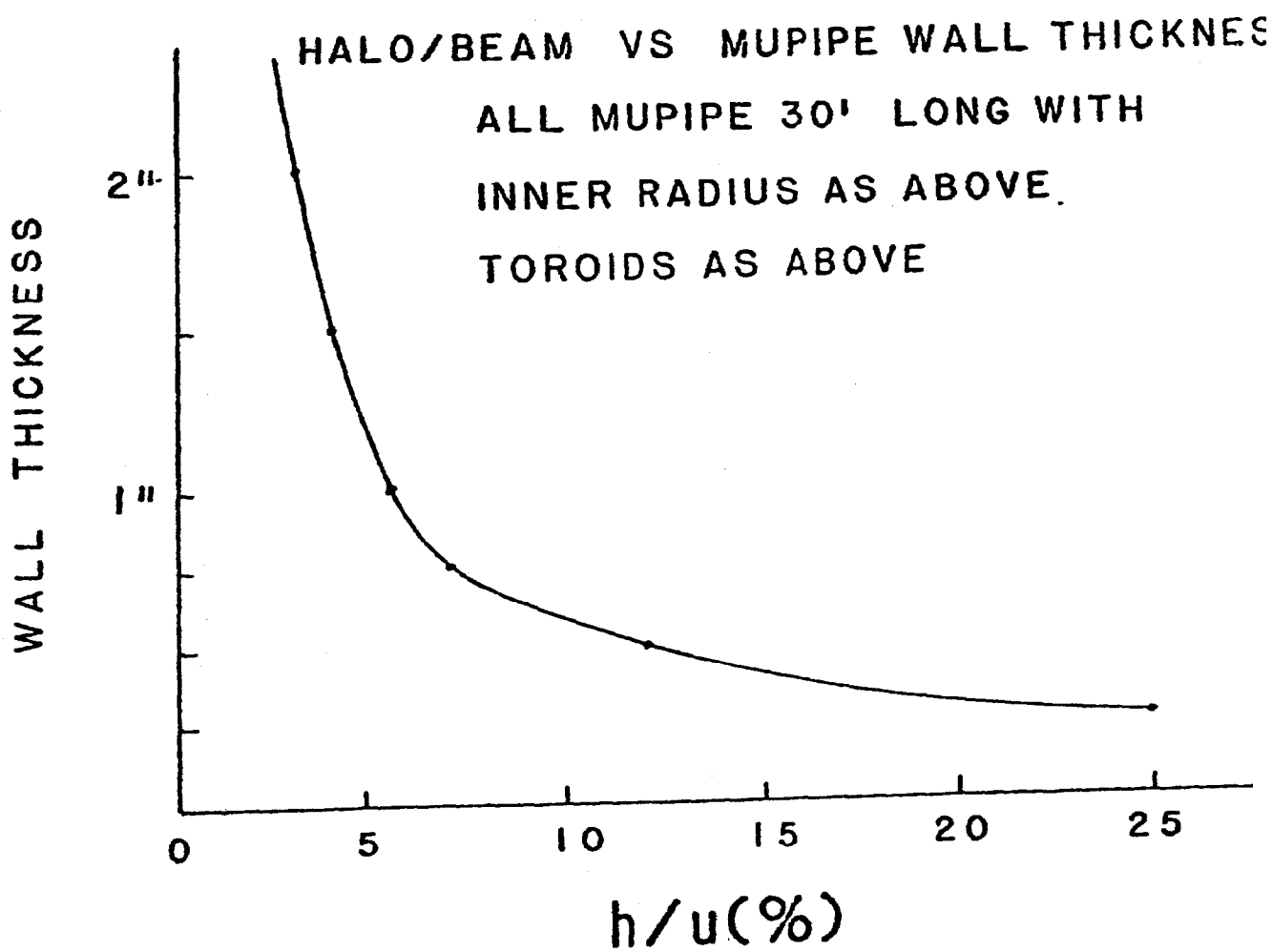
HALO/BEAM VS MUPIPE WALL THICKNES
ALL MUPIPE 30' LONG WITH
INNER RADIUS AS ABOVE.
TOROIDS AS ABOVE
WALL THICKNESS
2"
1"
0
5
10
15
20
25
h/u(%)

Figure 8.1-10

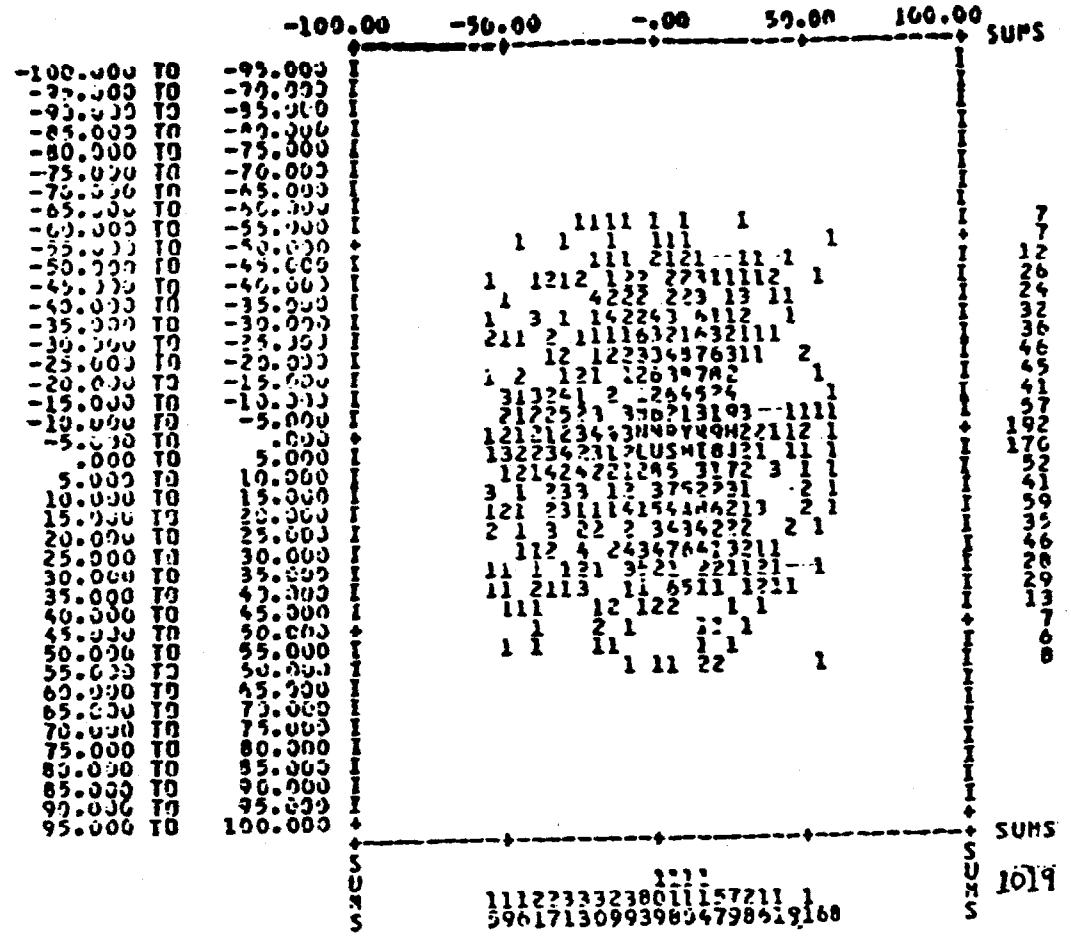

Plots below have the same vertical scale.

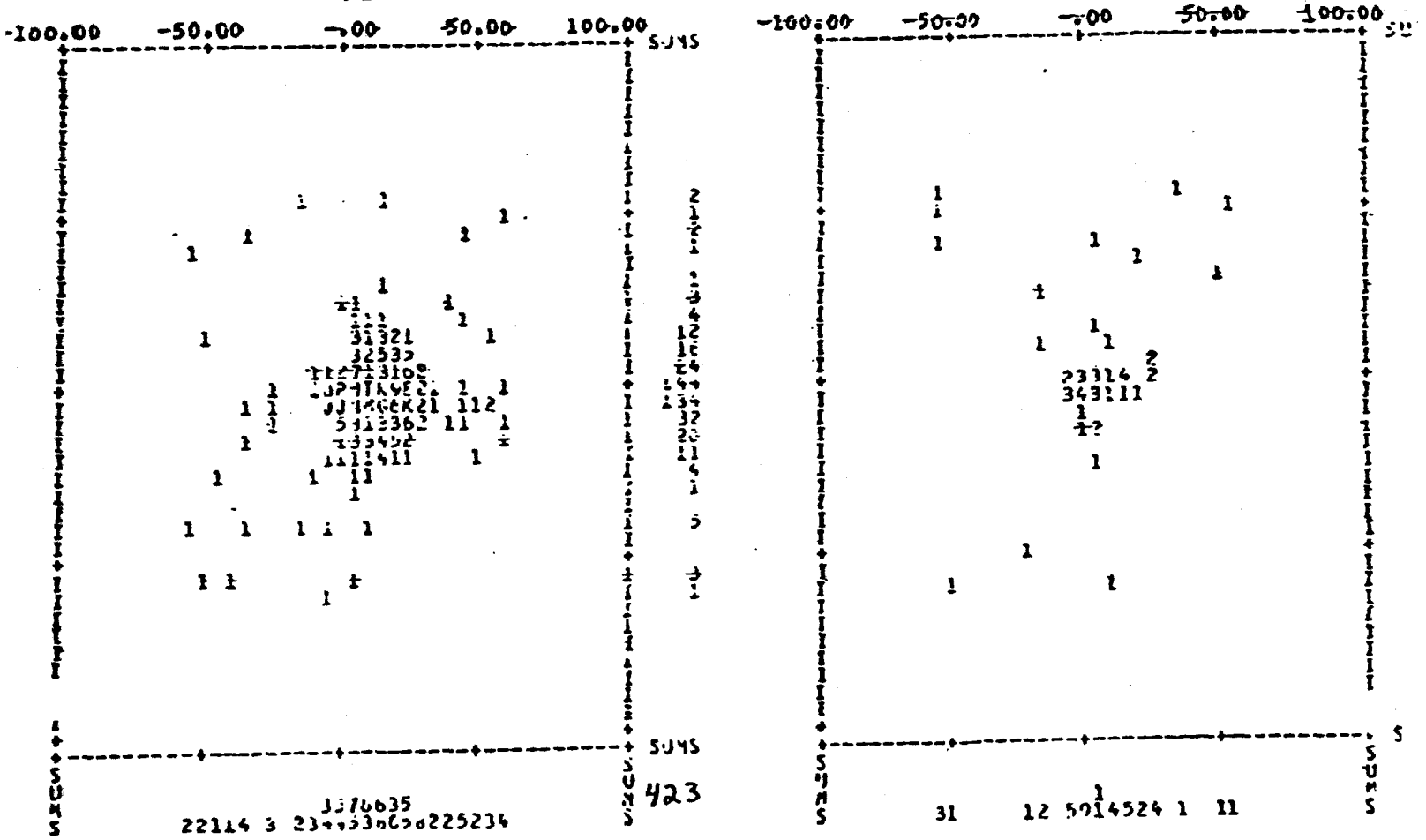

Figure 8.1-11

ELEVATION OF GROUND ALONG PATH OF MUON BEAM

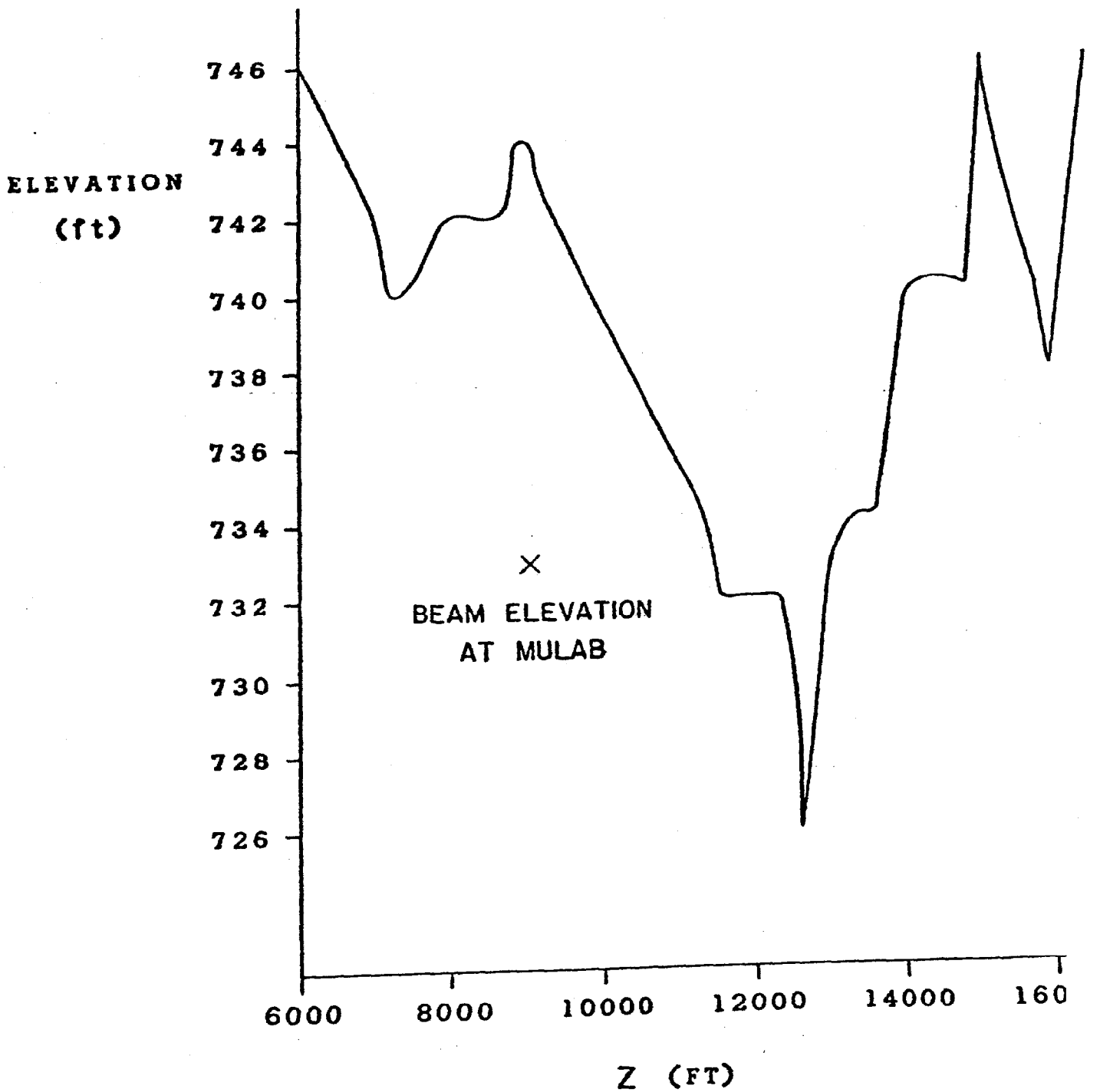

Figure 8.1-12

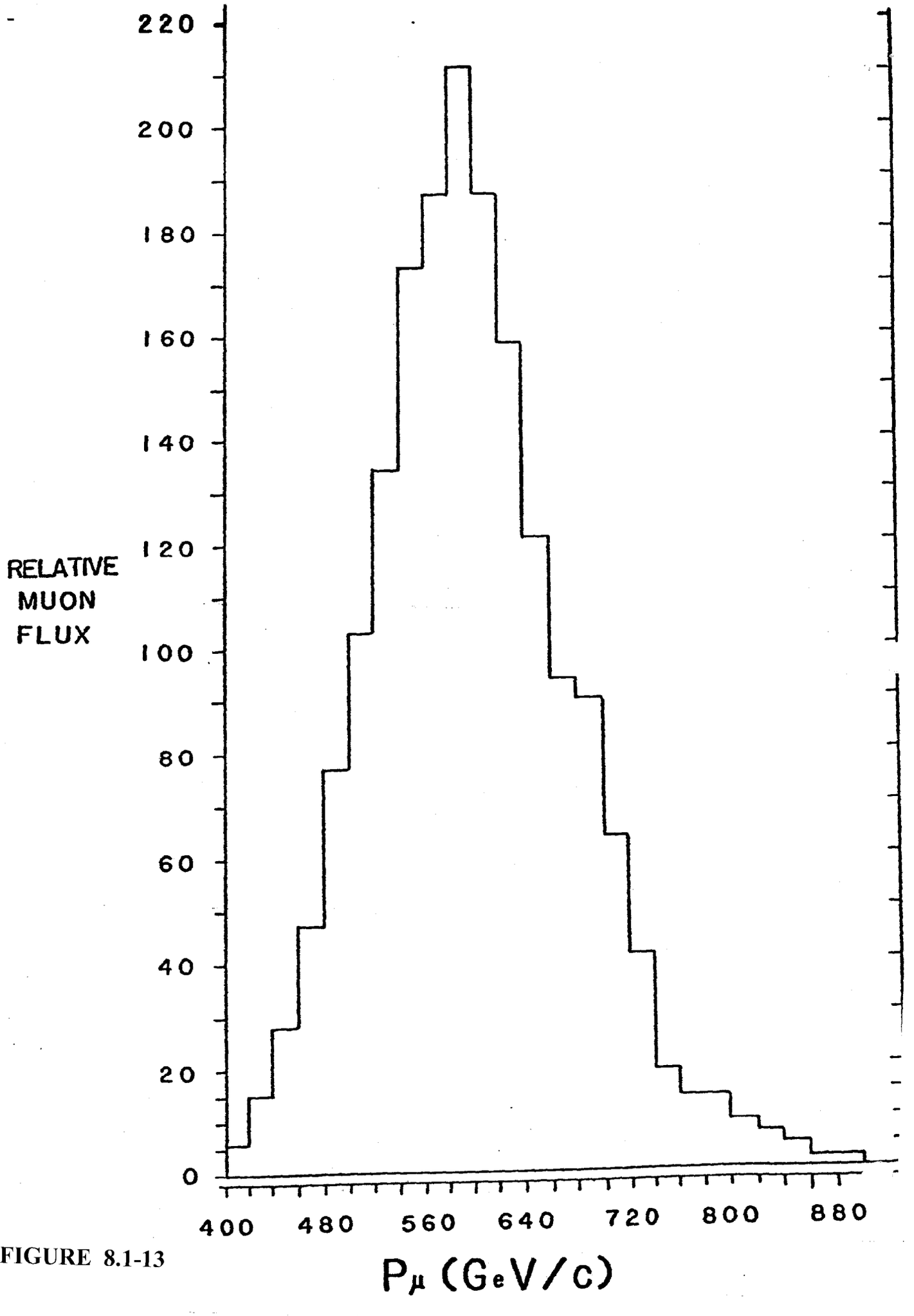
220
200
180
160
140
120
100
80
60
40
20
0
RELATIVE
MUON
FLUX
400
480
560
640
720
800
880
Pμ (GeV/c)

FIGURE 8.1-13

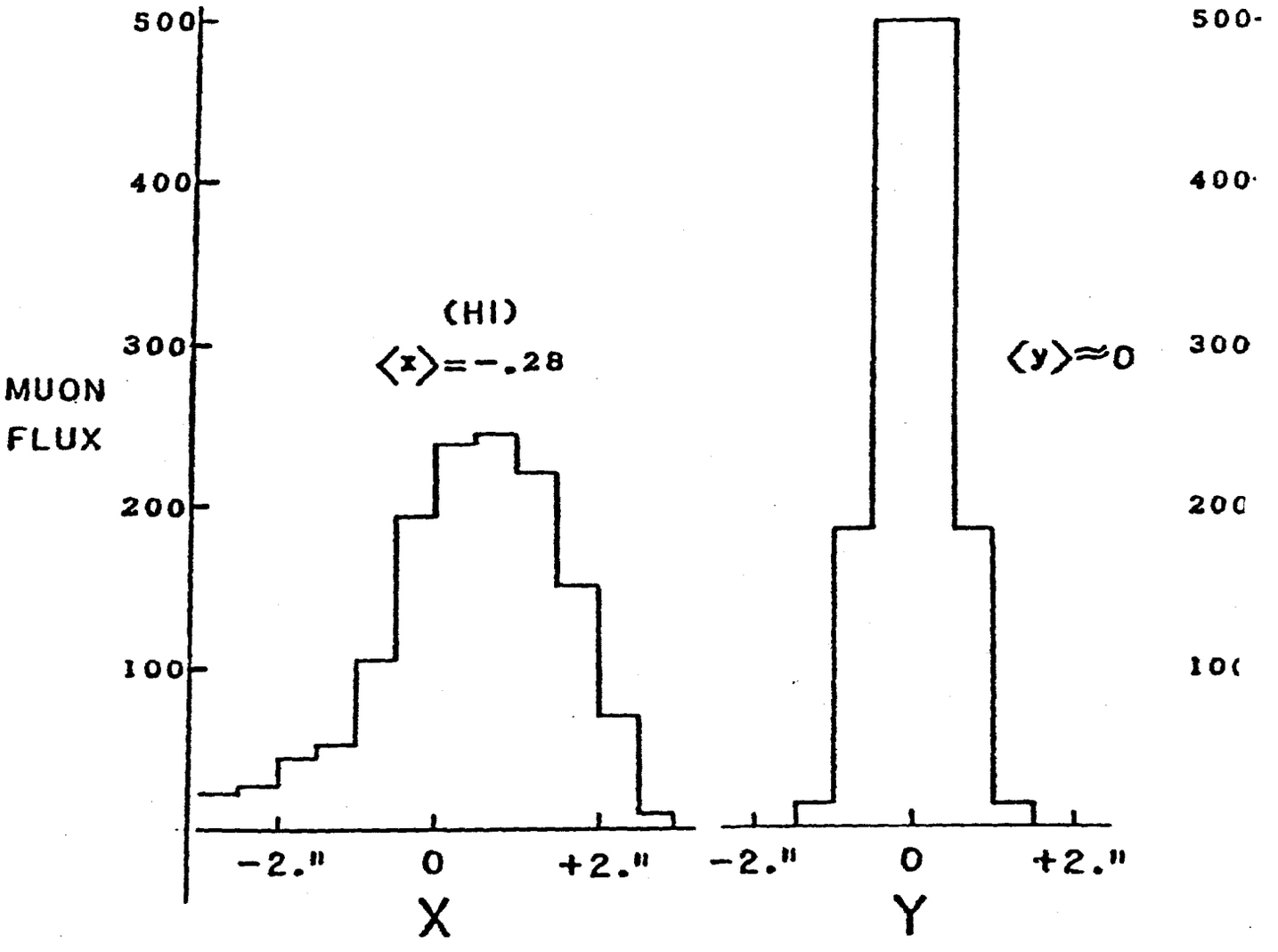

Figure 8.1-14

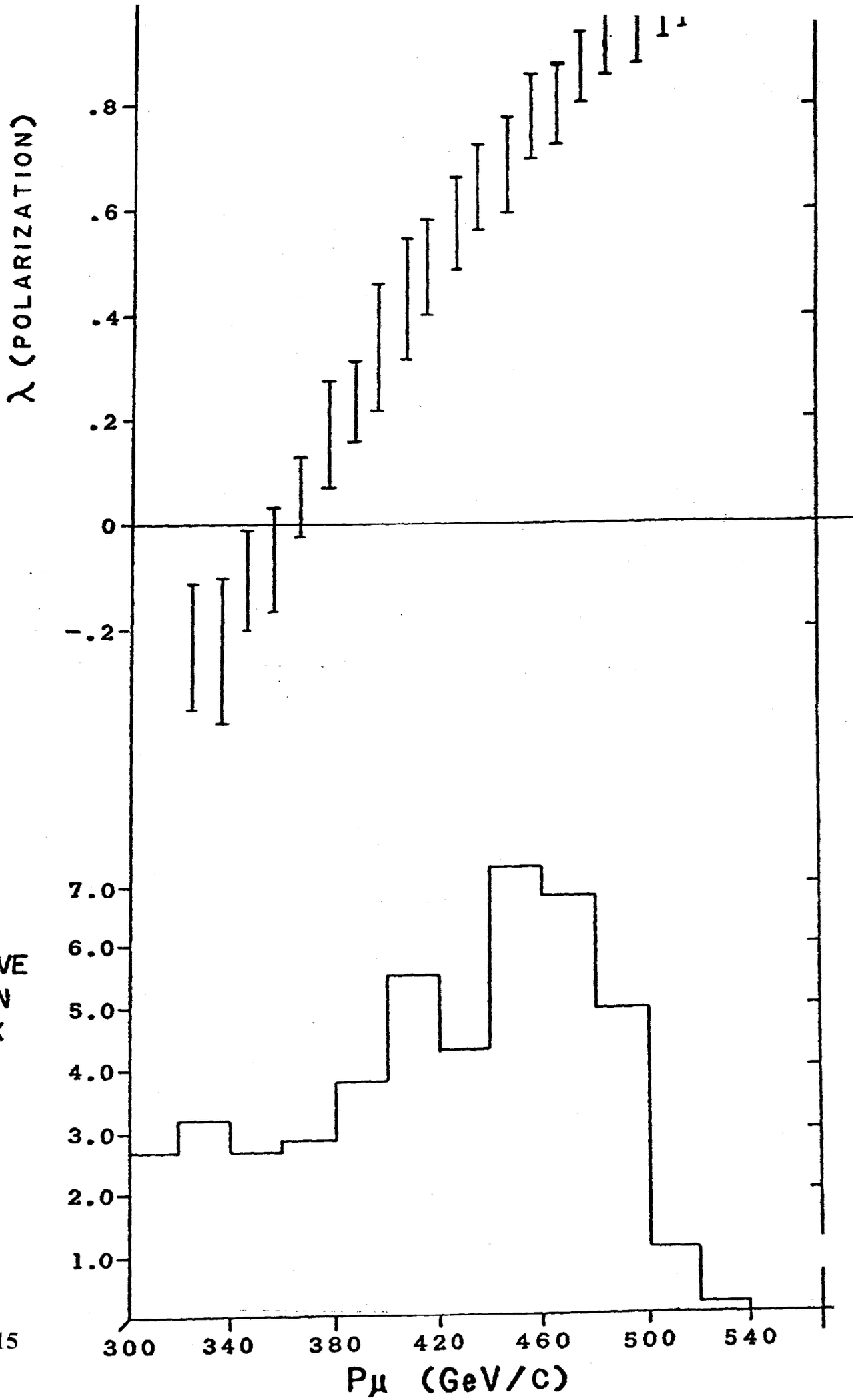
λ (POLARIZATION)
.8
.6
.4
.2
0
-.2
RELATIVE
MUON
FLUX
7.0
6.0
5.0
4.0
3.0
2.0
1.0
300
340
380
420
460
500
540
Pμ (GeV/C)

FIGURE 8.1-15

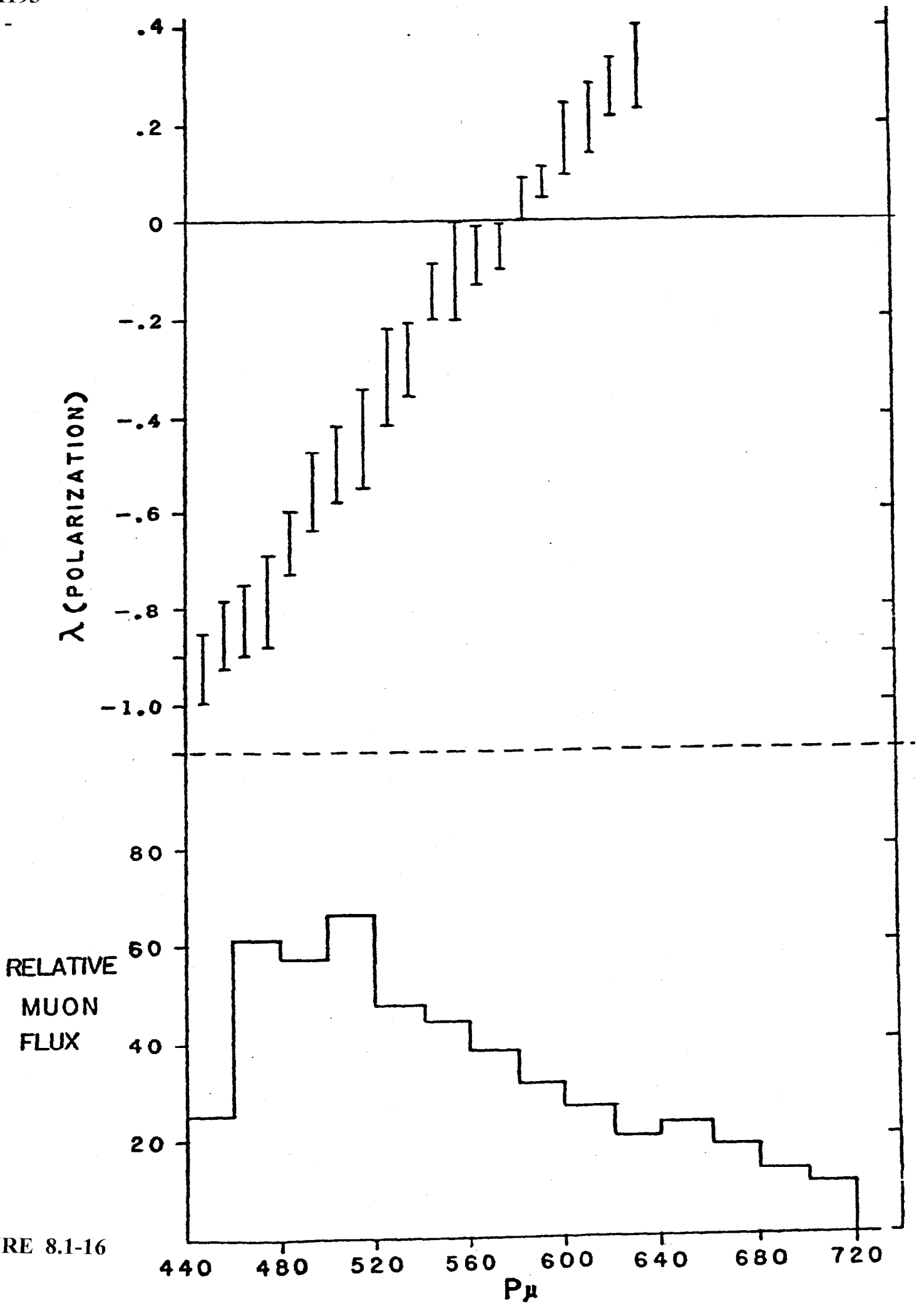
.4
.2
0
-.2
-.4
-.6
-.8
-1.0
λ (POLARIZATION)
80
60
40
20
RELATIVE
MUON
FLUX
440
480
520
560
600
640
680
720
Pμ

FIGURE 8.1-16

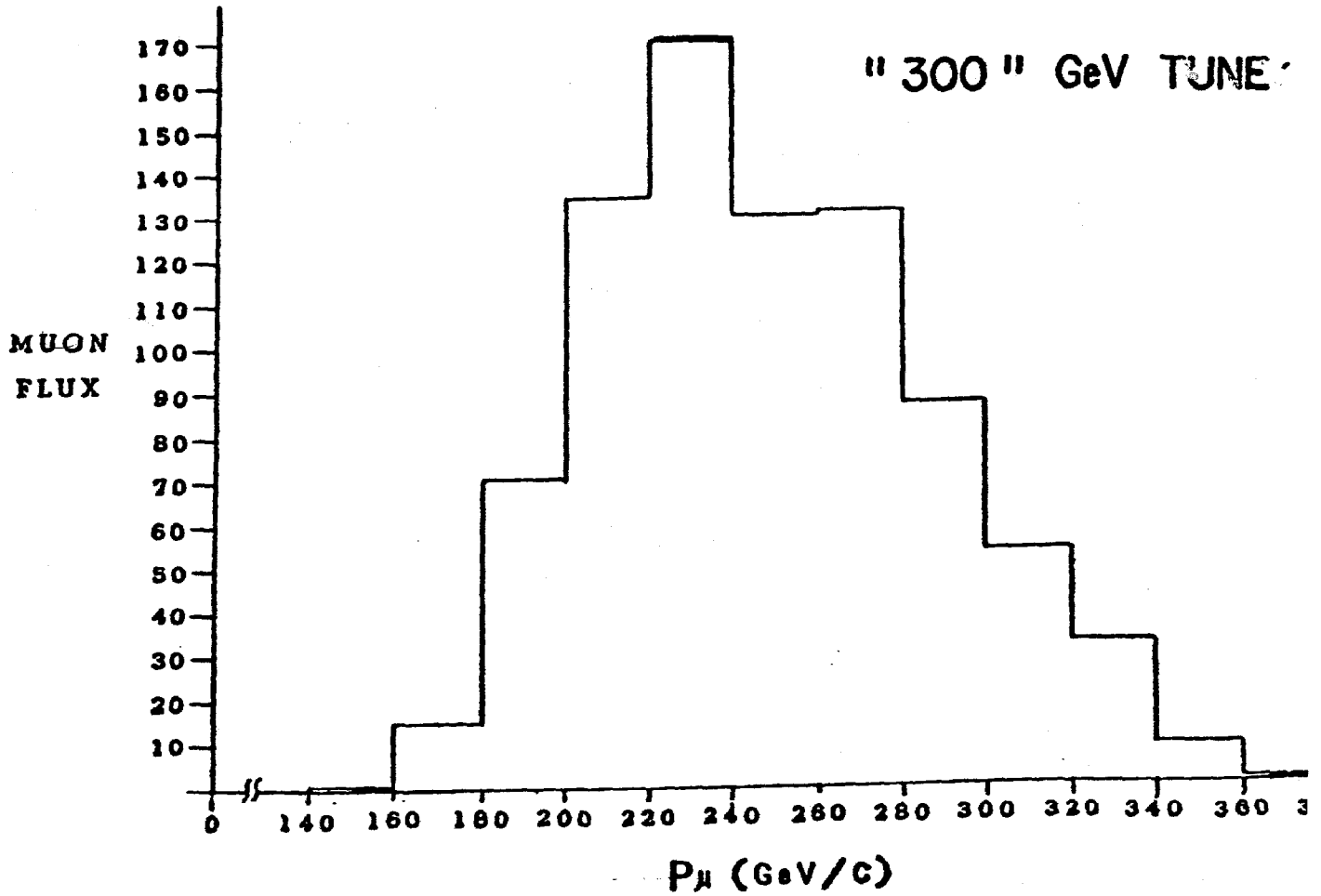
"300" GeV TUNE
MUON FLUX
170
160
150
140
130
120
110
100
90
80
70
60
50
40
30
20
10
0
140
160
180
200
220
240
260
280
300
320
340
360
Pμ (GeV/C)

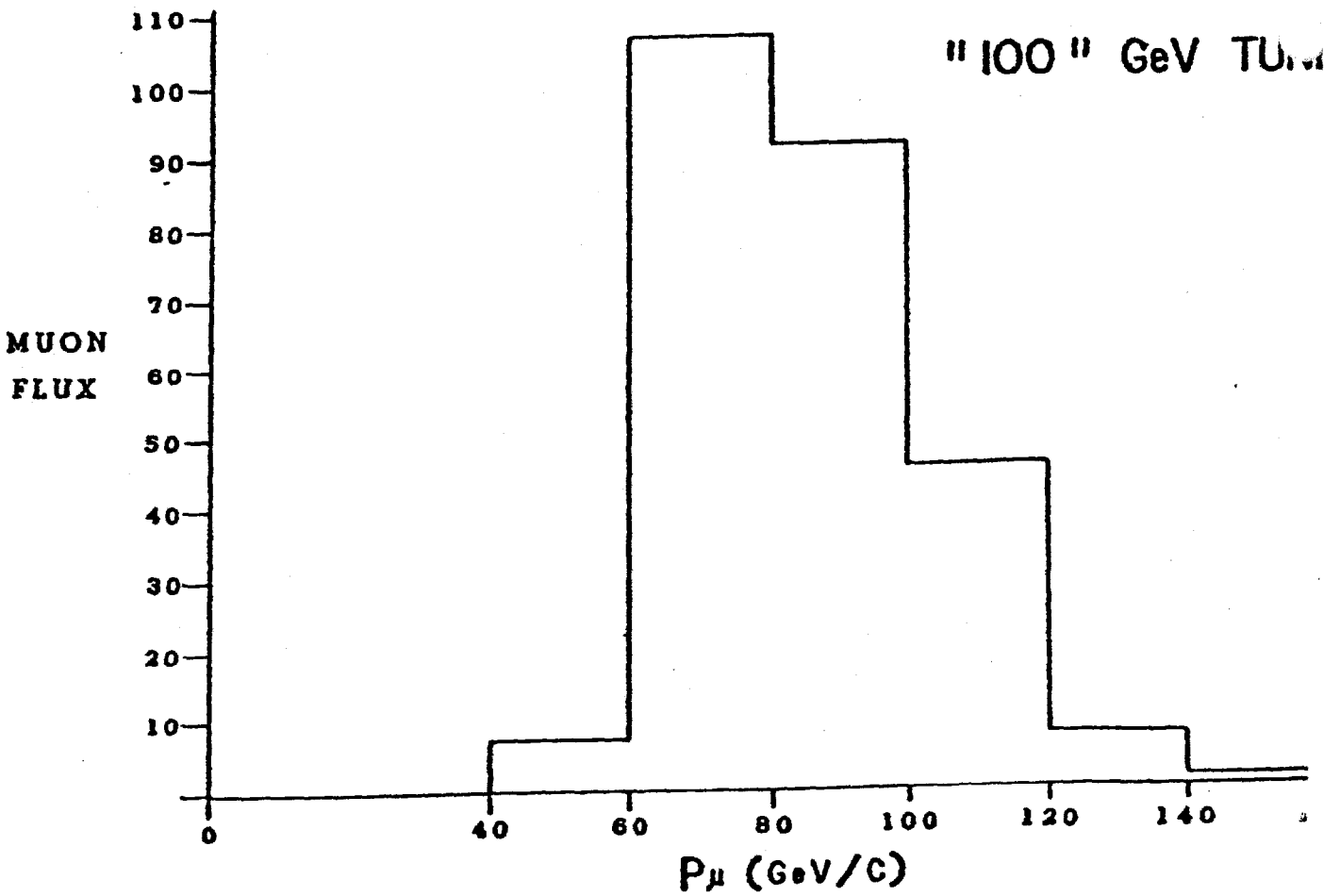
"100" GeV TU
MUON FLUX
110
100
90
80
70
60
50
40
30
20
10
0
40
60
80
100
120
140
Pμ (GeV/C)

Figure 8.1-17

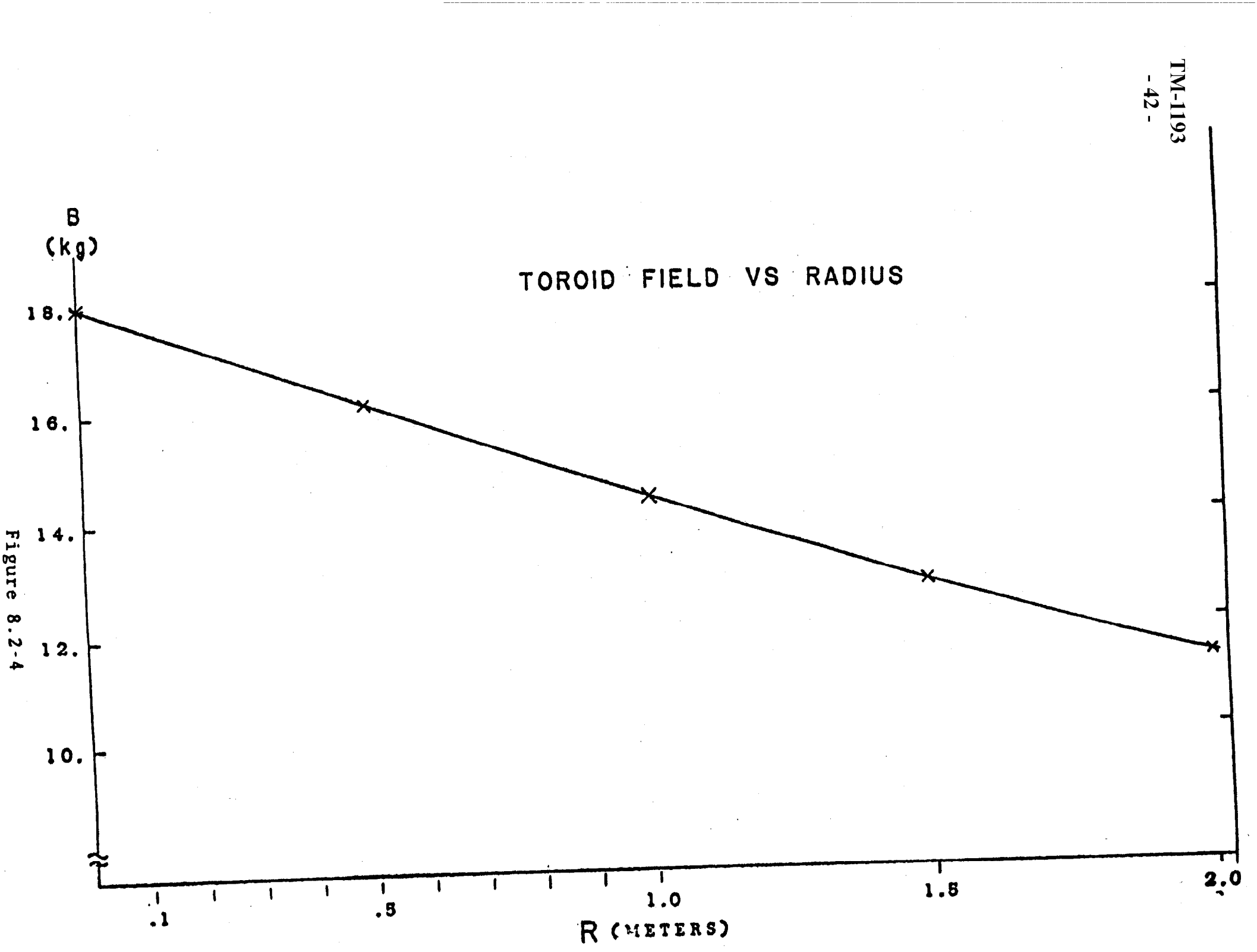

Figure 8.2-4

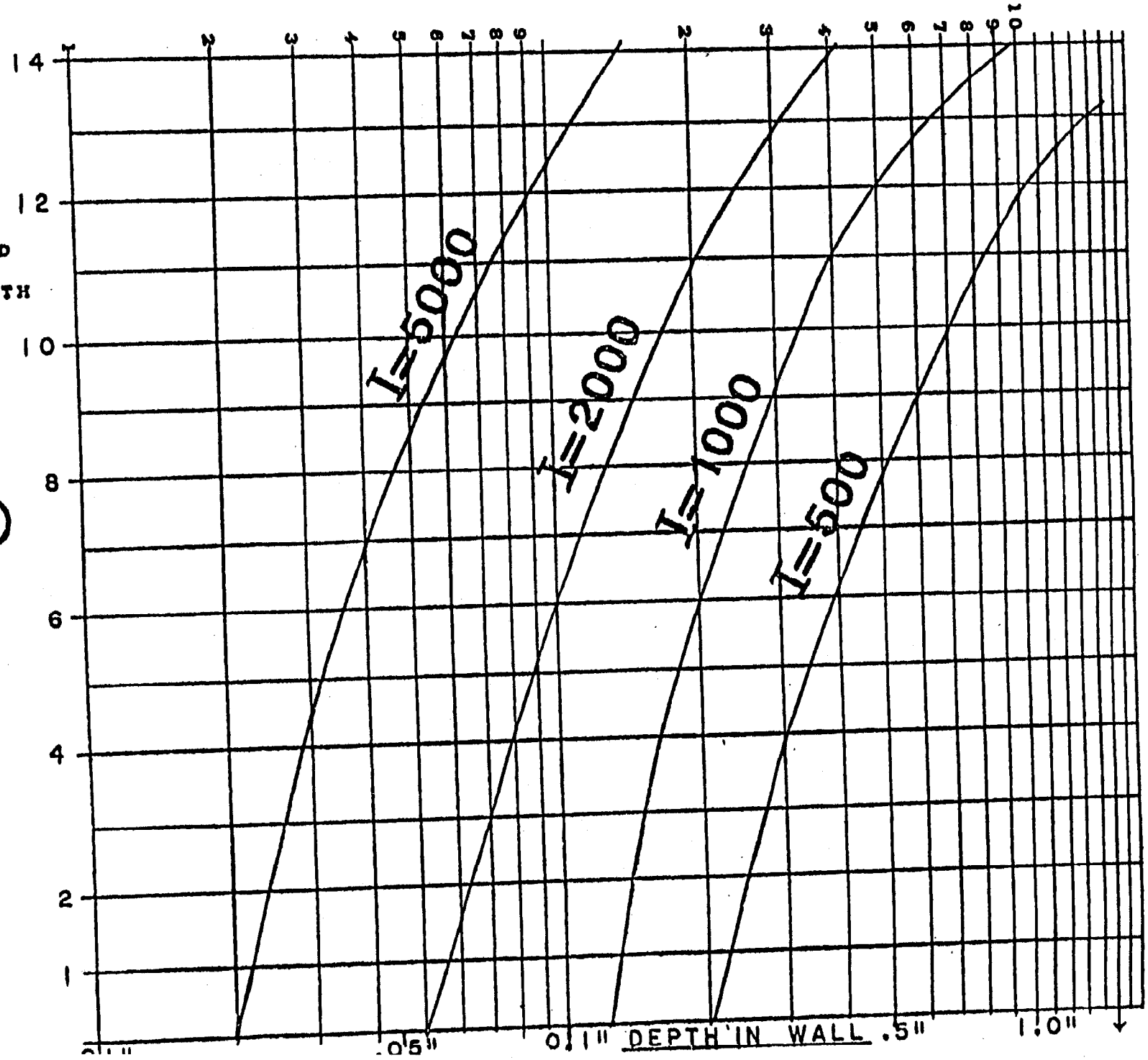
MUPIPE FIELD
VS WALL DEPTH
B
(kg)
14
12
10
8
6
4
2
1
I=5000
I=2000
I=1000
I=500
.05"
0.1" DEPTH IN WALL .5"
1.0"

Figure 8.2-5

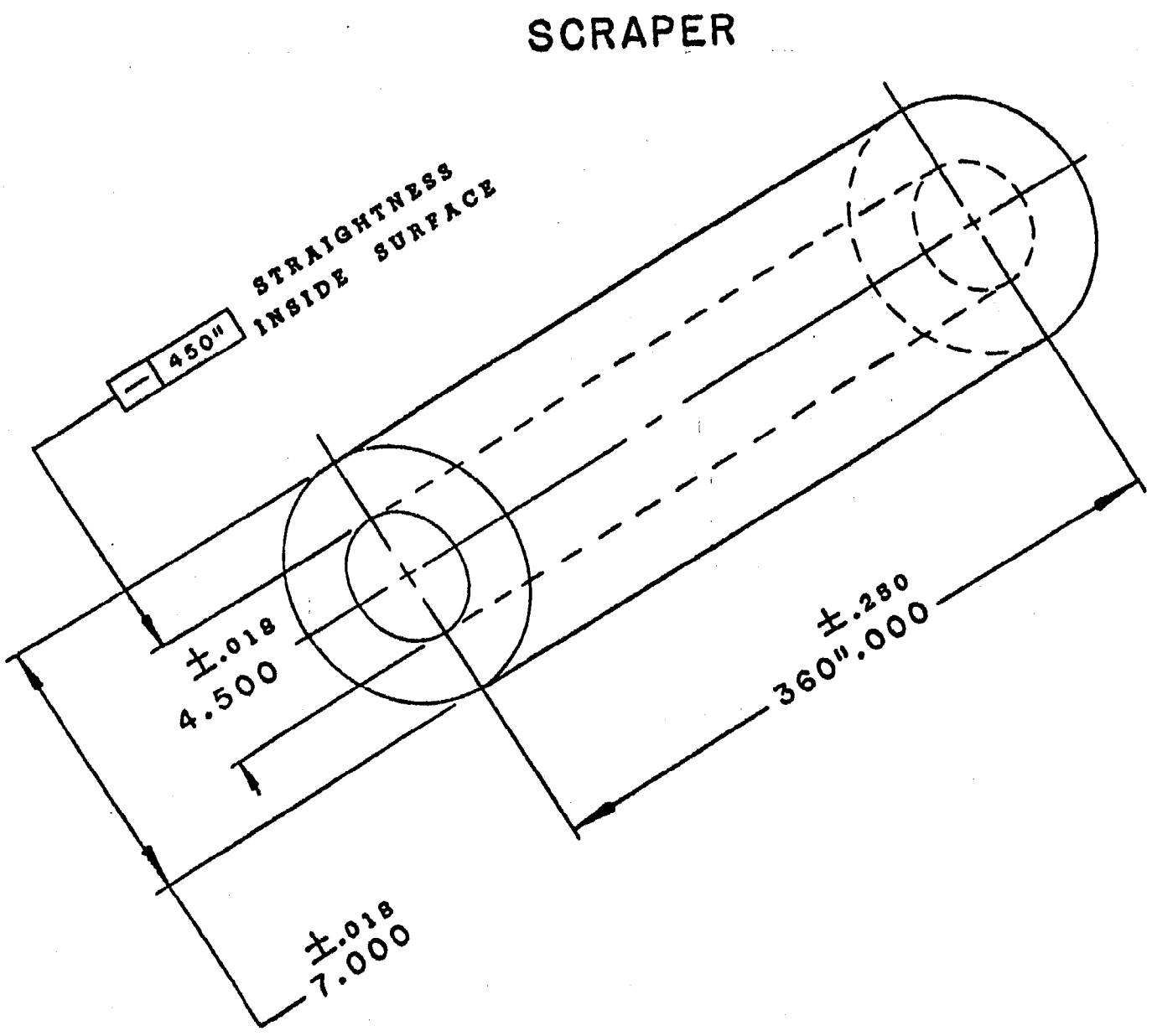
SCRAPER
STRAIGHTNESS
INSIDE SURFACE
.450"
±.018
4.500
±.250
360".000
±.018
7.000

Figure 8.2-6

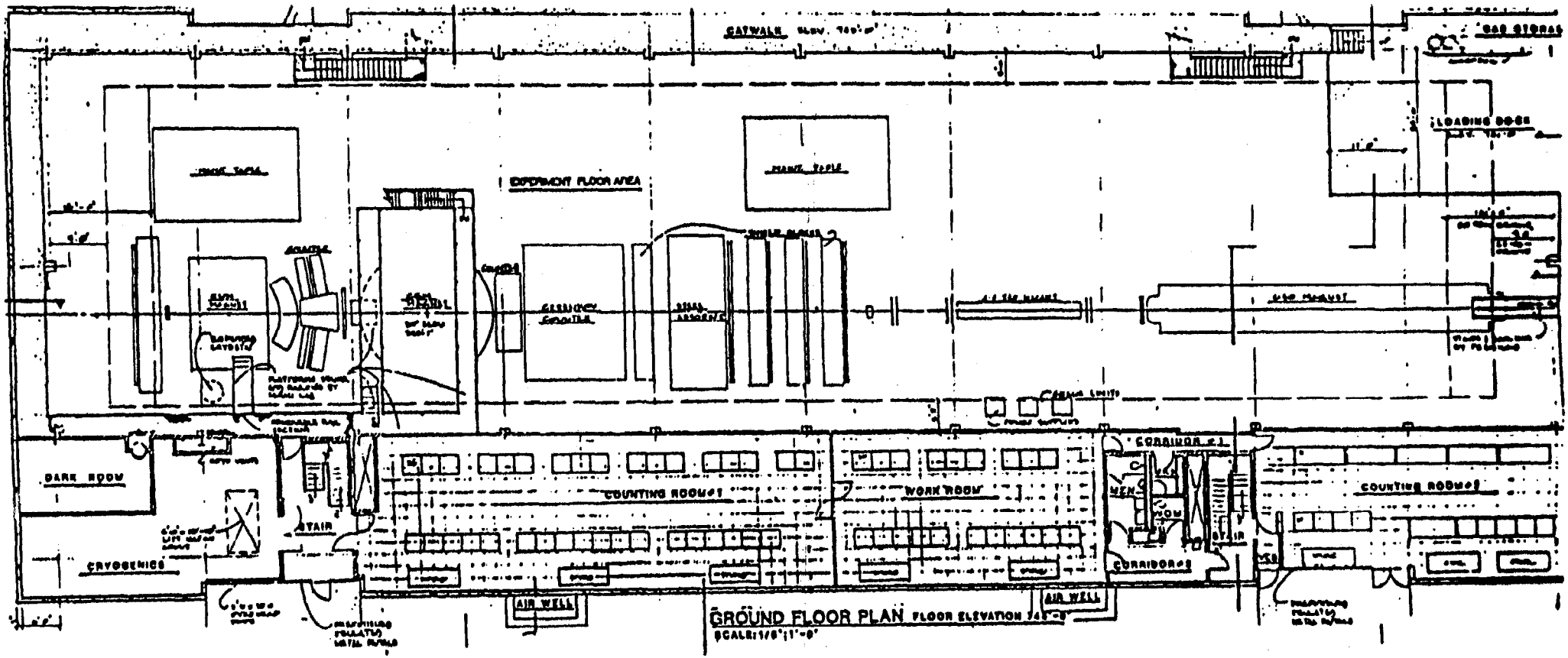

Muon Laboratory

Figure 8.3-7